# LAND COVER CLASSIFICATION IN A HETEROGENEOUS ENVIRONMENT: TESTING THE PERFORMANCE OF MULTISPECTRAL REMOTE SENSING DATA AND THE RANDOM FOREST ENSEMBLE ALGORITHM

**By**

**Kuhle Siseko Ndyamboti**

**Supervisor: Professor Onisimo Mutanga**

Submitted in fulfilment of the academic requirements for the degree of Master of Science in the Discipline of Geography in the

School of Agriculture, Earth and Environmental Sciences, College of Agriculture, Engineering and Science

University of KwaZulu-Natal, Pietermaritzburg

November 2013

## DECLARATION 1

This study was undertaken in fulfilment of an MSc in Environmental Science and represents the original work of the author. Any work taken from other authors or organizations is duly acknowledged within the text and reference list.

………………………… ..................................

Signature (Student) Date

Kuhle Ndyamboti

………………….……. ..................................

Signature (Supervisor) Date

Professor Onisimo Mutanga

**DECLARATION 2 – PUBLICATIONS**

DETAILS OF CONTRIBUTION TO PUBLICATIONS that form part of and/or include research presented in this thesis (includes publications in preparation and those that have been submitted, are in press or are published, and gives details of the contributions of each author to the experimental work and writing of each publication).

> **Publication 1**: Ndyamboti, K. S.[1], Mutanga, O.[2], Adam, E. M.[3] (In review). Assessing the utility of SPOT-5 data and the Random Forest ensemble algorithm to classify land use/cover in a complex environment.

The work was done by the first author under the guidance and supervision of the second and third authors.

> **Publication 2**: Ndyamboti, K. S.[1], Mutanga, O.[2], Slotow, R.[4] (In preparation). Discriminating spectrally similar land use/cover classes using WorldView-2 imagery in KwaZulu-Natal, South Africa.

The work was done by the first author under the guidance and supervision of the second and third authors.

[1], [2], [3] School of Agriculture, Earth and Environmental Science, College of Agriculture, Engineering and Science, University of KwaZulu-Natal, Pietermaritzburg, Private Bag X01, Scottsville, 3209, South Africa.

[4] School of Life Sciences, College of Agriculture, Engineering and Science, University of KwaZulu-Natal, Durban, P. Bag X54001, South Africa

# DEDICATION

To my mother

## PLAGIARISM DECLARATION

I, ………………………………….............. declare that;

1. The research reported in this thesis, except where otherwise indicated is my original work.
2. This thesis has not been submitted for any degree or examination at any other university.
3. This thesis does not contain other persons' data, pictures, graphs or other information, unless specifically acknowledged as being sourced from other persons.
4. This thesis does not contain other persons' writing, unless specifically acknowledged as being sourced from other researchers. Where other written sources have been quoted, then:
    a. Their words have been re-written, and the general information attributed to them has been referenced.
    b. Where their exact words have been used, then their writing has been placed in italics and inside quotation marks, and referenced.
5. This thesis does not contain text, graphics or tables copied and pasted from the internet, unless specifically acknowledged, and the source being detailed in the thesis and reference sections.

Signed: ……………………………………..

**TABLE OF CONTENTS**

## LIST OF FIGURES

## LIST OF TABLES

## ACRONYMS AND ABBREVIATIONS

| | |
|---|---|
| BS | Bare soil |
| CS | Coastal sand |
| DN | Digital number |
| ENVI | Environment for Visualizing Images |
| EU | *Eucalyptus grandis* |
| FLAASH | Fast Line-of-Sight Atmospheric Analysis of Spectral Hypercubes |
| GL | Grassland |
| GPS | Global Positioning System |
| HAT | Hawth’s Analysis Tools |
| IF | Indigenous forest |
| KZNPLULC | KwaZulu-Natal Provincial Land use/ Land cover |
| LIDAR | Light Detection and Ranging |
| LULC | Land use/ Land cover |
| ML | Maximum Likelihood |
| MS | Mature sugarcane |
| NIR | Near-infrared |
| OA | Overall accuracy |
| OC | Ocean |
| OOB | Out of bag |
| PA | Producer’s accuracy |
| PLSDA | Partial Least Squares Discriminant Analysis |
| PS | *Pinus* |
| QUAC | Quick Atmospheric Correction |

| | |
|---|---|
| RF | Random Forest |
| RGB | Red Green Blue |
| RMSE | Root Mean Square Error |
| RV | River |
| SANSA | South African National Space Agency |
| SAR | Synthetic Aperture Radar |
| SM | Settlements |
| SNR | Signal Noise Ratio |
| SPOT | System Probatoire d'Observation de la Terre |
| SVM | Support Vector Machines |
| SWIR | Shortwave-infrared |
| TM | Thematic Mapper |
| UA | User's accuracy |
| WT | Wetlands |
| YS | Young sugarcane |

## UNITS OF MEASUREMENT

| | |
|---|---|
| % | Percent |
| ° | Degree |
| °C | Degrees Celsius |
| cm | Centimetre |
| km | Kilometre |
| $km^2$ | Square kilometre |
| m | Meter |
| nm | Nanometer |
| µm | Micrometer |

# ABSTRACT

Land use/land cover (LULC) information is essential for a plethora of applications including environmental monitoring and natural resource management. Traditionally, field surveying techniques were the sole source of acquiring such information; however, these methods are labour intensive, costly and time consuming. With the advent of remote sensing, LULC information can be acquired in an economical, less tedious and non-time consuming manner at shorter temporal cycles and over larger areas. The aim of this study was to assess the utility of multispectral remote sensing data and the Random Forest (RF) algorithm to improve accuracy of LULC maps in heterogeneous ecosystems.

The first part of this study used moderate resolution SPOT-5 data to compare the performance of the RF algorithm to that of the commonly used Maximum Likelihood (ML) classifier. Results indicated that RF performed significantly better than ML (66.1%) and yielded an overall accuracy of 80.2%. Moreover, RF variable importance measures were able to provide an insight on the bands that played a pivotal role in the classification process. Due to the fact that moderate resolution satellite data was used, both classifiers seemed to experience some difficulties in discriminating amongst classes that exhibited similar spectral responses such as *Eucalyptus grandis* and *Pinus* tree plantations, young sugarcane and mature sugarcane, as well as river and ocean water. In that regard, the next section attempted to address this shortfall.

The second part of the study used high resolution multispectral data acquired from the WorldView-2 sensor to discriminate amongst six spectrally similar LULC classes using the advanced RF algorithm. Results suggested that the use of WorldView-2 data together with the RF ensemble algorithm is a robust and accurate method for separating classes exhibiting similar spectral responses. The classification process yielded an overall accuracy of 91.23% and also provided valuable insight into WorldView-2 bands that were most suitable for discriminating the LULC categories.

Overall, the study concluded that: (i) multispectral remote sensing data is an effective tool for obtaining accurate and timely LULC information, (ii) moderate resolution multispectral data can be used to map broad LULC categories whereas high resolution multispectral data can

be used to separate LULC at finer levels of detail, (iii) RF is a robust and effective tool for producing LULC maps that are less prone to error.

## ACKNOWLEDGEMENTS

I would like to express my sincere gratitude to the following individuals for playing a crucial role in ensuring that this dissertation was completed successfully:

Firstly, I would like to thank God for granting me the opportunity and strength to pursue and complete my Masters degree within the minimum required time, to him I would like to say "Heavenly father I am grateful".

Secondly, thanks must go to Professor Onisimo Mutanga for being such an encouraging and supportive supervisor throughout the course of my Masters degree. Prof Onnie, I would like to thank you for teaching me the art of scientific writing and dedicating your time to providing valuable comments and suggestions that ensured this dissertation is what it is today.

To Dr Elhadi Adam, I am extremely thankful for the insight you gave me on how to perform my analysis.

A very special thank you must also go to the Applied Centre for Climate and Earth Systems Science (ACCESS) for granting me funding for the research.

I extend my gratitude to my mother and the rest of the Ndyamboti family for believing in me and encouraging me through tough times.

Finally, to my friends, fellow master's students, and the rest of the Environmental Sciences and Geography Department, I am extremely grateful for the overwhelming support and love shown to me during this special time of my life. Meeting and interacting with each and every one of you was a true blessing.

# CHAPTER 1

# INTRODUCTION

## 1.1 Background

Reliable and timely land use/land cover (LULC) information is essential to many government and private organizations for different applications such as environmental monitoring, transportation planning, urban development, and modeling of ever-changing landscapes (Chen and Stow, 2003). Furthermore, reliable information on the current state of LULC has become increasingly important as nations plan to combat problems associated with the destruction of important wetlands, loss of prime agricultural lands, deteriorating environmental quality and the loss of fish and wildlife habitats (Ozdemir and Karnieli, 2011). Prior to the existence of space-borne satellite sensors, conventional land-surveying techniques were commonly used to acquire such information (Comber *et al.*, 2004; Chapman *et al.*, 2009). Despite the relatively high accuracy achieved through these techniques, they are often expensive, time consuming and labor intensive. Remotely sensed satellite imagery, on the other hand, provides a cheaper, timely and less tedious alternative to conventional techniques and covers larger areas at high temporal frequencies (Friedl and Brodley, 1997; Kavzoglu and Colkesen, 2009; Mathur and Foody, 2008; Huang *et al.*, 2002).

Over the years, a large number of satellite sensors have been utilized for thematic mapping with varying degrees of success. Notably, multispectral datasets such as Landsat and SPOT have been among the most commonly used owing to their longer historical records (Ojo and Adesina, 2010). However, traditional multispectral sensors face a limitation as they typically collect data using only few broad wavelengths from the visible to the infrared regions of the spectrum (Dye *et al.*, 2011). The broad wavelengths result in limited discrimination capabilities when objects with subtle differences such as different types of the same species, are to be detected (Melgani and Bruzzone, 2004). Recent studies have shown that high classification accuracy can be achieved through the use of hyperspectral remote sensing datasets (Chan and Paelinckx, 2008b;

Petropoulos *et al.*, 2012a; Ham *et al.*, 2005). In contrast to broadband multispectral imagery, these datasets provide hundreds of bands within the visible, near infrared (NIR) and shortwave-infrared (SWIR) regions of the spectrum that allow better discrimination among similar ground-cover classes (Adam *et al.*, 2012; Peerbhay *et al.*, 2013; Mansour *et al.*, 2012). However, although hyperspectral image data provide a wealth of information, the data present some difficulties, such as increased image costs, data volumes, data redundancy and data processing costs (Dye *et al.*, 2011; Melgani and Bruzzone, 2004; Ham *et al.*, 2005). This has driven researchers to explore alternative satellite datasets that have the potential to overcome the shortcomings of highly dimensional hyperspectral datasets. The WorldView-2 sensor has particularly caught the attention of the remote sensing community.

WorldView-2 offers a high number of spectral bands (8 bands) and fine spatial resolution (2 m) than conventional multispectral sensors, while reducing unnecessary repetition of information as contained in hyperspectral data (Mutanga *et al.*, 2012). In addition to the four traditional bands (Blue, Green, Red and NIR-1), WorldView-2 contains four new bands (Coastal blue, Yellow, Red-edge and NIR-2) that are currently unavailable in other sensors with sub-meter spatial resolution (Immitzer *et al.*, 2012; Novack *et al.*, 2011; Zhou *et al.*, 2012). Each of these bands is specifically configured to a specific region of the electromagnetic spectrum that is sensitive to a particular feature on the ground, enabling successful detection of slight variations in ground-cover objects (Ozdemir and Karnieli, 2011; Ribeiro and Garcia Fonseca, 2013). However, despite the immense potential of WorldView-2 as a source of producing reliable thematic maps, studies on LULC classification have so far been limited to urban environments (Novack *et al.*, 2011; Zhang and Kerekes, 2011; Ribeiro and Garcia Fonseca, 2013). Results from these studies showed that the availability of the new bands in the WorldVeiw-2 sensor significantly improved the accuracy of classification maps in homogeneous urban landscapes. The question therefore remains whether the new bands in the WorldVeiw-2 sensor can better the classification accuracy in heterogeneous rural environments.

The use of high resolution multispectral imagery, however, does not necessarily guarantee high classification accuracy as classification accuracy is largely dependent on the classifier employed for the classification (Lu and Weng, 2007; Hermes *et al.*, 1999; Mountrakis *et al.*, 2011). Several classification techniques have been developed and applied to remote sensing imagery. Popular methods include classical pattern recognition techniques such as K-nearest neighbor, minimum distance to means, maximum likelihood and linear discriminant analysis. (Kavzoglu and Colkesen, 2009; Song *et al.*, 2005; Tan *et al.*, 2011; Perumal and Bhaskaran, 2010). These classifiers are generally characterized by having an explicit underlying probability model such as the Gaussian normal distribution, and their performance depends on how well the data correlate with the pre-defined model (Pal and Mather, 2004; Ghose *et al.*, 2010). More recently, however, machine learning classifiers have emerged as more accurate and effective replacements for standard parametric classifiers, and have been shown to improve classification accuracy in coarse resolution datasets(Watanachaturaporn *et al.*, 2008; Sesnie *et al.*, 2010). Specifically, one machine learning method that has shown great potential in remote sensing image classification is Random Forest (RF).

Random Forest can be considered as an improvement of conventional ensemble methods such as boosting and bagging (Walton, 2008; Chan and Paelinckx, 2008a). In the remote sensing domain, it has been successfully used for the classification of a wide range of datasets including multispectral (Pal, 2005; Mutanga *et al.*, 2012), hyperspectral (Ham *et al.*, 2005), Light Detection and Ranging (LIDAR) (Guo *et al.*, 2011), synthetic aperture radar (SAR) (Loosvelt *et al.*, 2012), as well as aerial imagery (Chapman *et al.*, 2009). RF employs a bagging-based approach to form an ensemble of classification trees (Watts *et al.*, 2009). Each of the trees within the ensemble is trained on a subset of the original training samples (Waske *et al.*, 2009; Sesnie *et al.*, 2010). Approximately one third of the training samples are set aside to form an external dataset known as the out-of-bag (OOB) dataset (Chan *et al.*, 2012; Loosvelt *et al.*, 2012). This dataset (OOB) acts a measure of accuracy that produces results comparable to external accuracy assessments, so long as there is no bias in the reference data (Watts *et al.*, 2009). RF also uses the OOB samples to calculate an internal measure of variable importance that gives an indication of the most useful variables in the classification (Dye *et al.*, 2011; Dye *et al.*, 2012).

Furthermore, RF is superior to many tree-based algorithms as it is not sensitive to noise or overtraining, and is also capable of handling unbalanced data sets (Watts and Lawrence, 2008). It is also simpler to use than other tree-based algorithms as it only requires two user-defined parameters: the number of trees grown (*ntree*), and the number of variables used to split each node (*mtry*) (Adam *et al.*, 2009; Mansour *et al.*, 2012). It is in light of this, that this dissertation sets itself to the following aims and objectives.

## 1.2 Aims and Objectives

The aim of this study was to assess the utility multispectral remote sensing data and the Random Forest (RF) algorithm to accurately map land use/land cover (LULC) in a heterogeneous environment. The main objectives were as follows:

(i) TO EXAMINE THE UTILITY OF MODERATE RESOLUTION SPOT-5 DATA TO CLASSIFY LULC IN AN ECOSYSTEM CONSISTING OF DIVERSE LULC CATEGORIES.

(ii) TO EVALUATE THE EFFICIENCY OF HIGH RESOLUTION WORLDVIEW-2 IMAGERY IN THE CLASSIFICATION OF SPECTRALLY SIMILAR LULC CLASSES.

(iii) TO RANK THE IMPORTANCE OF SPOT-5 AND WORLDVIEW-2 BANDS IN CLASSIFYING LULC CATEGORIES USING THE RF VARIABLE IMPORTANCE MEASURES.

## 1.3 Outline of thesis

This thesis is presented in four chapters. However, it is structured mainly around two core chapters (Chapter Two and Three) that form publishable papers and will be submitted to peer reviewed journals. Since both these chapters have detailed sections covering the study area, literature review, and methodology, these sections are not dealt with in the introductory section of the thesis in order to avoid redundance.

Chapter Two assesses the capability of moderate resolution multispectral data to classify land use/land cover (LULC) in a heterogeneous ecosystem using the advanced Random Forest (RF) algorithm as well as the well-known Maximum Likelihood (ML) method. The RF variable importance measures are then used to determine the SPOT-5 wavelengths that played a pivotal role in the landscape classification process.

Chapter Three, on the other hand, evaluates the effectiveness of high resolution WorldView-2 multispectral data in discriminating spectrally similar LULC categories in the study area using the RF ensemble algorithm. Once again, the variable importance measures of RF are used to determine the bands that play a significant role in the classification of the spectrally similar LULC classes.

Chapter Four provides a synthesis of the study. The aims and objectives of the study are discussed in detail while important findings from the study are highlighted. The chapter also examines the limitations of this study and presents recommendations for future research.

CHAPTER 2

# Assessing the utility of SPOT-5 data and the Random Forest ensemble algorithm to classify land use/cover in a complex environment

## 2.1 Abstract

The present study sought to assess the ability of SPOT-5 data to accurately map land use/land cover (LULC) in a heterogeneous environment using the advanced Random Forest (RF) algorithm as well as the commonly used Maximum Likelihood (ML) classifier. Results showed that SPOT-5 data can successfully discriminate amongst broad LULC classes using both classifiers. However, finer classes with minimal spectral variability could not be adequately differentiated. A comparison between the two classifiers showed that RF yielded better results, and also provided meaningful insight into wavelengths that were most useful in the classification process. Overall, the study demonstrated the unprecedented ability of RF to accurately classify LULC objects relative to conventional statistical classifiers.

**Keywords:** SPOT-5; land use/cover classification; Random Forests; Maximum Likelihood; comparison

## 2.2 Introduction

Land use/land cover (LULC) is dynamic in nature and is an important factor for understanding the interaction of anthropogenic activities with the environment (Mahdavi, 2010). Furthermore, LULC data is among the most important and most universally used terrestrial datasets (Loveland *et al.*, 2000). Scientists and government agencies need timely and accurate LULC information for a variety of applications such as natural resource management (Foody and Mathur, 2004a), environmental monitoring (Chen and Stow, 2003), and ecological monitoring of vegetation communities (Pal and Mather, 2004). Without this information, policymakers often fail to make decisions or make incorrect decisions (Haack and English, 1996).

Traditionally, LULC maps were derived from field surveys with GPS receivers, manual human interpretation on hard-copy maps or aerial photographs (Anderson *et al.*, 1976; Yuan *et al.*, 2005). However, the conventional methods based on fieldwork are usually expensive, time consuming, labor intensive, and often lack the necessary geometric accuracy (Li and Shao, 2012). Remote sensing offers a practical and economical means to mapping LULC, especially over large areas (Mathur and Foody, 2008). New satellite-borne instruments collect data in the visible and infrared portions of the spectrum at resolutions ranging from a few meters to a kilometer, presenting unique benefits for the detection of Earth surface materials (Kavzoglu, 2009). The rapid improvement in remote sensing technologies have been propelled by three interconnected aspects, namely, advances in sensor technology and data quality, improved and standardized remote sensing methods, and research applications (Rogan and Chen, 2004). The advances in remote sensing technology have also resulted in the development of hyperspectral sensors.

The potential of hyperspectral sensors to offer more discrimination amongst similar Earth surface objects has long been highlighted by earlier researchers (Bazi and Melgani, 2006; Ham *et al.*, 2005; Melgani and Bruzzone, 2004). These sensors capture spectral reflectance from ground-cover objects in a number of narrow continuous spectral bands, acquiring an enormous amount of spectral information (Petropoulos *et al.*, 2012b). The rich and detailed spectral data can be used to detect a large range of surface objects which cannot be identified by multispectral sensors (Ham *et al.*, 2005). However, as hyperspectral sensors provide added spectral information, they also carry new challenges such as the "curse of dimensionality", also known as the Hughes effect (Bazi and Melgani, 2006; Chan and Paelinckx, 2008b). The high inter-band correlations and the need to determine multiple parameters contribute to the problems of classifying hyperspectral data (Pal, 2006). As a result, hyperspectral datasets have gained only limited acceptance for operational use, and many researchers opt for multispectral data for the classification of LULC (Loveland *et al.*, 2000; Mariz *et al.*, 2009; Perumal and Bhaskaran, 2010; Song *et al.*, 2012; Immitzer *et al.*, 2012; Pal, 2005; Ozdemir and Karnieli, 2011; Salberg and Jenssen, 2012; Sesnie *et al.*, 2010).

Depending on the spectral and spatial properties of the multispectral sensor used, the amount of classification accuracy attained varies significantly (Lu and Weng, 2007). If coarse resolution multispectral data is used (spatial resolution > 250m), analysis is generally limited to discerning between forested and non-forested areas, as coarse-resolution data is well suited for discriminating broad categories of LULC (Rogan and Chen, 2004). Moderate resolution satellites like Landsat, with spatial resolutions of 15-30m, can classify forests, grasslands and urban surfaces using the different spectral reflectance of each object, however, finer details cannot be reliably differentiated at these resolutions (Peters *et al.*, 2011). In the recent decade, researchers have advocated for the use of high resolution sensors such as Quickbird and Ikonos, as these sensors allow the generation of geometrically detailed LULC maps (Mariz *et al.*, 2009; Moran, 2010). Another advantage of these high resolution sensors is that they greatly reduce the mixed-pixel problem which is common in coarse resolution datasets, thus providing a greater potential to extract much more detailed information on LULC structures (Lu and Weng, 2005; Moran, 2010).

High resolution multispectral data however comes at a relatively high cost, hence, LULC maps at regional levels are usually based on medium-resolution satellite data such as Landsat Thematic Mapper (TM) and SPOT imagery (Fang *et al.*, 2006). Incidentally, SPOT-4 satellite data has recently been used for the mapping of LULC in KwaZulu-Natal owing to its lower cost, longer history and higher frequency of archives (Ezemvelo, 2005). Unfortunately, the relatively coarse spatial (10m) and spectral resolution (4 bands) of SPOT-4 data means that LULC maps derived from SPOT-5 data are often judged to be insufficient in quality and thus not trustworthy for quantitative environmental applications, especially in complex (Manandhar *et al.*, 2009). Recent studies have however argued that unreliable LULC maps result from the use of traditional per-pixel classifiers (Foody and Mathur, 2004a). A vast number of LULC maps are generated using traditional per-pixel classifiers such as minimum distance and linear discriminant analysis (Ghose *et al.*, 2010). These traditional classifiers cannot effectively handle complex landscapes as well as the mixed pixel problem and therefore produce LULC maps that are prone to error (Lu and Weng, 2004).

Over the years, some advanced techniques such as Random Forests (RF) have been introduced to overcome the shortcomings of statistical classifiers and produce improved classification performance. Recent comparisons suggest that these advanced non-parametric methods are superior to conventional parametric methods for LULC classification (Dixon and Candade, 2008; Pal and Mather, 2004; Song *et al.*, 2012). However, none of the above mentioned comparisons have been conducted in an area characterized by landscape heterogeneity such as St Lucia, in the coastal areas of Eastern South Africa. Hence, the objective of this study was to compare the efficiency of the advanced RF algorithm and the commonly used Maximum Likelihood algorithm to classify LULC in a heterogeneous environment using moderate resolution (10 m) SPOT-5 data. Such a comparison is crucial as it enables environmental managers to make the correct decision in terms of selecting the appropriate classifier to use for generating reliable LULC maps. Moreover, the study sought to bridge the gap between previous studies by focusing on breaking down broad Level I classes (Commercial forest plantations and Sugarcane fields) into less complex Level II classes (*Eucalyptus grandis* and *Pinus* tree plantations; Young sugarcane and Mature sugarcane).

## 2.3 Materials and Methods

### 2.3.1 Study area

The study area (Figure 1) is situated near St Lucia (28°22’21’’S and 32°24’52’’E), a small coastal town located in the KwaZulu-Natal province of South Africa. St Lucia lies 275 km north of the city of Durban and falls under the Mtubatuba Local Municipality. This town experiences a subtropical climate and has a mean annual temperature of 21.5°C (Feleke, 2010). Approximately

1200-1300mm of rain falls per annum and almost 60% of the annual rain falls during the summer months (Mafuratidze, 2010). The study site covers an area of approximately 136 $km^2$ and is characterised by a number of LULC types. The south-western part of the study site is used for agricultural purposes and consists mostly of sugarcane fields. The south-eastern part, on other hand, is covered almost entirely by indigenous forest, whereas the north-eastern part consists mostly of natural growing vegetation. Towards the north western part of the study site, commercial forest plantations dominate. These plantations are owned by Mondi SA, a paper manufacturing company.

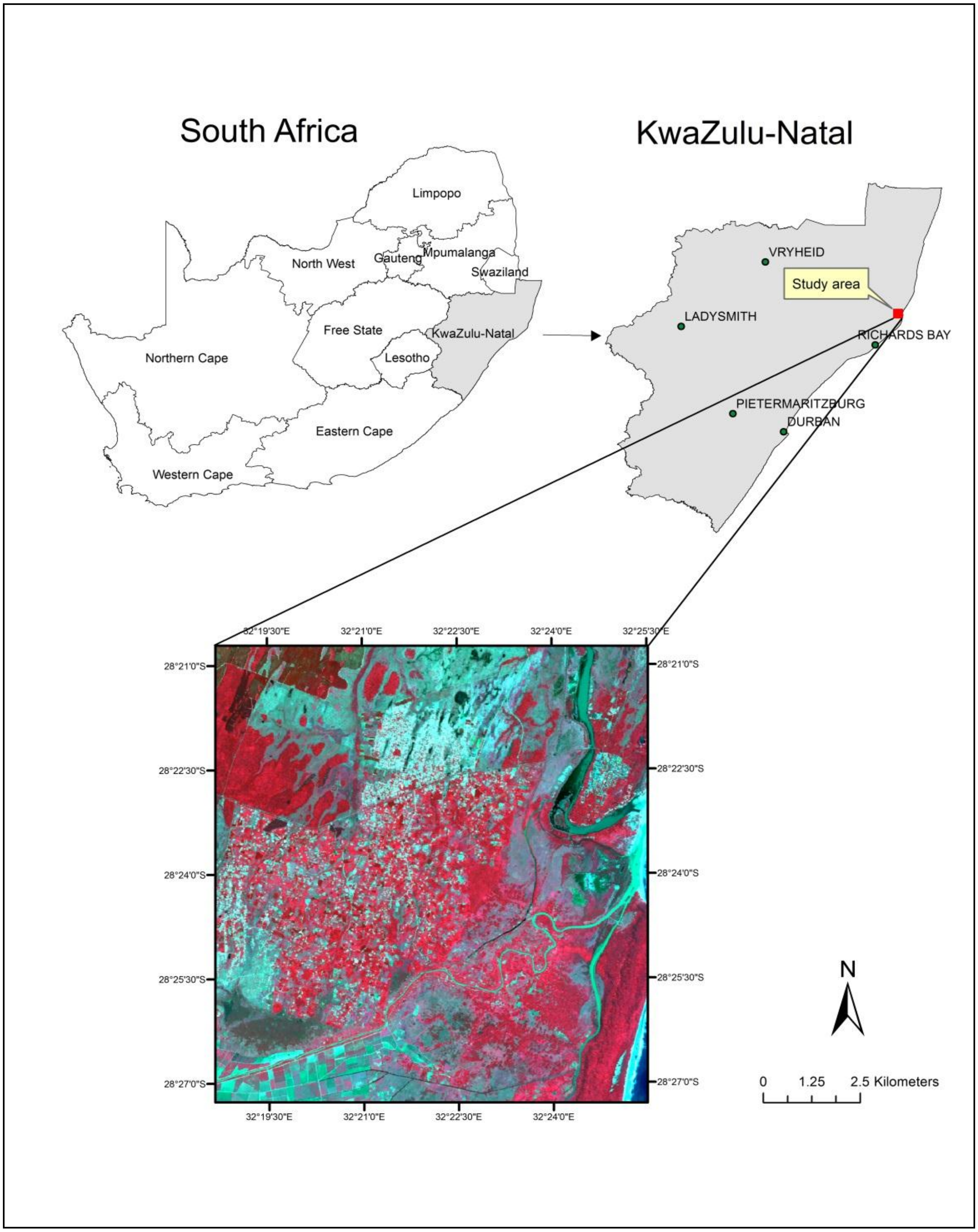


**Figure 1**. Location of the study area in relation to the rest of South Africa and KwaZulu-Natal. An insert of a SPOT-5 (RGB=123) satellite image is provided.

### 2.3.2 Data acquisition and pre-processing

Satellite imagery of the study site was captured on 23 May 2011 under cloudless conditions by the SPOT-5 multispectral sensor. The image consisted of four bands with a spatial resolution of 10 m with the exception of the Shortwave-Infrared (SWIR) band (20 m). The spectral ranges of the four bands were: Green (0.5 – 0.59 µm), Red (0.61 – 0.68 µm), Near-infrared (0.78 – 0.89 µm), and SWIR (1.58 – 1.75 µm). The image was then orthorectified using georeferenced high resolution aerial photographs of St Lucia based on 20 ground control points. Using the 1$^{st}$ order polynomial transformation technique, an overall Root Mean Square Error (RMSE) of 0.28% of a pixel was achieved. A visual assessment confirmed that the RMSE (0.28%) was sufficient as the image was aligned perfectly with the ancillary data (aerial photographs). Thereafter, the Fast Line-of-Sight Atmospheric Analysis of Spectral Hypercubes (FLAASH) algorithm built into Environment for Visualizing Images (ENVI) 4.7 image processing software was used to atmospherically correct the image as described in the software package. Digital numbers (DNs) were converted to top-of-atmosphere reflectance using updated sensor calibration coefficients for SPOT-5 data provided by the SANSA thereby allowing retrieval of accurate reflectance spectra (Duro *et al.*, 2012).

### 2.3.3 Field data acquisition

Using Hawth's Analysis Tools (HAT) in ArcGIS 9.3 software, random points (n = 1080) were generated on a LULC map of the study area extracted from the KwaZulu-Natal Provincial LULC (KZNPLULC) map. The KZNPLULC map was developed in 2006 based on SPOT-4 satellite imagery and is available to the public at no cost from the following website: http://bgis.sanbi.org/kzn/landcover.asp. The points were then uploaded into a global positioning system (GPS) and used to navigate to the field sites. Once the sample point was located in the field, a 10× 10 m plot was created to cover a homogenous area of the LULC class and a GPS reading was then taken. Broad Level I classes such as Commercial forest plantations and Sugarcane fields were broken down into less complex Level II classes with the aid of ancillary data. For commercial forest plantations, the ancillary data was in the form of a forest stand map containing species data on all the plantations present in the study area. The map suggested that four distinct species of *Pinus* tree plantations occurred: *Pinus elliottii, Pinus taeda, Pinus oocarpa* and *Pinus caribaea*, whereas only two species of *Eucalyptus grandis* plantations were present: *Eucalyptus grandis* (*Urophylla* hybrid) and *Eucalyptus grandis* (*Camaldulensis* hybrid). For that reason, the commercial forest plantations were broken down into *Eucalyptus grandis* plantation and *Pinus* tree plantation. For sugarcane fields however, each field was classified as Young Sugarcane or Mature Sugarcane based on known planting. Additional reference data for locations that could not be accessed due to limiting factors such as rugged terrain were obtained by visually interpreting high resolution aerial photographs (0.5 m) of St Lucia. Thereafter, the HAT extension in ArcGIS 9.3 was used to randomly split the points into a training (70%) and validation (30%) dataset. The splitting of the datasets was performed three times in an effort to minimize any potential bias. Training data were used to optimize the RF classification and to train the prediction model, whereas the validation data were used to test the quality and reliability of the prediction model (Mutanga *et al.*, 2012).

### 2.3.4 Classifiers

The Maximum Likelihood (ML) classifier is the most commonly used supervised method in remote sensing and is based on Bayesian probability theory (Kavzoglu and Colkesen, 2009; Richards, 2006). Maximum Likelihood assumes that the statistics for each category have normal distribution and determines the possibility that each pixel belongs to a specific class (Mingjie *et al.*, 2010). Unless the user selects a probability threshold, all pixels are classified and allocated to the LULC category that has the greatest likelihood. Maximum Likelihhod was utilized in this study as it is often used as a baseline for comparing machine learning classifiers (Wulder and Franklin, 2003). The Random Forests (RF) classifier on the other hand, is an ensemble algorithm developed in the field of machine learning that uses a similar but improved method of bagging (Gislason *et al.*, 2006; Walton, 2008). This classifier operates by creating multiple classification and regression trees, each trained on a bootstrapped sample of the original training data (Loosvelt *et al.*, 2012).

Each tree created then casts a unit class vote, with the final classification determined by an amongst-tree plurality decision (Watts *et al.*, 2009; Peters *et al.*, 2011). For each of the new training sets that are created, approximately a third (1/3) of the samples are randomly left out, known as the out-of-bag (OOB) samples (Chan and Paelinckx, 2008b). The OOB samples are subsequently used for the calculation of an unbiased error rate as well as variable importance, eliminating the requirement for a test dataset (Prasad *et al.*, 2006; Peters *et al.*, 2007; Loosvelt *et al.*, 2012). Compared to other non-parametric classifiers, RF is not sensitive to noise (Watts and Lawrence, 2008), does not suffer from over-fitting or a long training time (Loosvelt *et al.*, 2012), and is computationally faster (Rodriguez-Galiano *et al.*, 2012a). Other key advantages of RF include its capability to determine variable importance (Rodríguez-Galiano *et al.*, 2012b), and handling unbalanced data sets (Watts *et al.*, 2009).

### 2.3.5 Optimization of RF parameters

The success of the RF classifier depends on the optimization of key parameters (*ntree* and *mtry*). The grid search method was therefore used to optimize the RF classifier using a 10-fold cross validation. The concept behind the grid search technique is that different pairs of parameters are evaluated and the one yielding the highest level of accuracy is selected (Kavzoglu and Colkesen, 2009). To establish the optimal value for the RF parameters, a number of experiments (n = 60) were carried out using different combinations of *ntree* and *mtry*. The experiments were carried out three times as the data was also split three times into a training (70%) and validation (30%) dataset. The value of *ntree* ranged between 500 and 10 000 using intervals of 500 while *mtry* was tested from 2 to 4 using intervals of 1.

### 2.3.6 Accuracy assessment

"A classification is not complete until its accuracy is assessed" (Lillesand *et al.*, 2008). Map users require accuracy information to indicate the quality of LULC maps and their suitability for a particular purpose (Foody, 2004). To determine the accuracy of the classification maps, a confusion matrix (Congalton, 1991) was built for each map and the Overall Accuracy (OA), User's Accuracy (UA), Producer's Accuracy (PA) were computed. OA refers to the number of pixels from the validation dataset that have been correctly classified over the total number of pixels used for the accuracy assessment and is expressed in percentage (Petropoulos *et al.*, 2012b). UA reflects the probability that a pixel belongs to a certain LULC class and the algorithm has labeled the pixel correctly into the same LULC class, whereas PA indicates the probability that the algorithm has properly allocated an image pixel (Petropoulos *et al.*, 2012a). The kappa index is the most widely used measure of assessing the amount of agreement between the reference and validation datasets (Foody, 2009a). However, this method is inadequate if the same sample sites are used as it assumes that samples employed for the classification are independent (Manandhar *et al.*, 2009). Moreover, kappa indices have fundamental conceptual flaws, such as being undefined even for simple cases (Pontius Jr and Millones, 2011). Due to the large number of limitations, Pontius Jr and Millones (2011) recommended that researchers abondone the use of kappa indices and replace these indices with a more useful and simpler approach that focuses on two components of disagreement between maps. The present study therefore used allocation disagreement and quantity disagreement measures as proposed by Pontius Jr and Millones (2011).

### 2.3.7 Statistical significance of classification results

In this study, the McNemar test was used to assess whether a statistically significant difference exists in the accuracies obtained by the two image classifiers. This is a non-parametric test that is based upon confusion matrices that are 2 by 2 in dimension (Foody, 2004). The test is based on the standardized normal test statistic.

$$Z = \frac{f_{12} - f_{21}}{\sqrt{f_{12} + f_{21}}} \tag{1}$$

Where $f_{12}$ represents the number of pixels that are incorrectly allocated by algorithm 1 but correctly allocated by algorithm 2, and $f_{21}$ indicates the number of pixels that are correctly allocated by algorithm 1 but incorrectly allocated by classifier 2 (Manandhar *et al.*, 2009;

Petropoulos *et al.*, 2012b). The analysis can also be based on a chi-square distribution as below. The square of ***Z*** follows a chi-squared distribution with one degree of freedom (Foody and Mathur, 2004a).

$$\chi^2 = \frac{(f12 - f21)^2}{f12 - f21} \quad (2)$$

Two classification outputs can be declared significantly different if ***Z*** is greater than 1.96 at 5% significance level (Foody, 2009b).

## 2.4 Results

### 2.4.1. Optimization of RF parameters

The RF parameters were optimized so as to determine the combination of parameters that yielded the lowest OOB error for each of the three randomly split datasets. The OOB estimate of error was used as a measure of assessing the prediction accuracy. Results showed that the lowest OOB error (22.75%) was produced by a combination of *ntree* and *mtry* values of 3500 and 2 respectively. The parameters were therefore selected to perform the final classification and generate the RF based classification map.  It was also discovered that the default value of *mtry* (n = 2), which is the square root of input variables (Mansour *et al.*, 2012), produced the lowest OOB error in each of the three calibration datasets.

### 2.4.2. RF variable importance

The RF variable importance was used to rank the importance of each of the SPOT-5 bands in the landscape classification process. Results showed that the near-infrared band was the most instrumental variable in the classification of the 12 LULC classes considered in this study (Figure 2A). The Red and Green bands on the other hand were ranked 2$^{nd}$ and 3$^{rd}$ respectively, whereas the Shortwave Infrared (SWIR) band was the least important variable in the classification. The results concerning the importance of SPOT-5 bands in discriminating individual LULC classes (Figure 2B), showed that the near-infrared band played a fundamental role in the classification of 6 out of the 12 classes considered in this study. These six classes were: Coastal Sand (CS), *Eucalyptus grandis* plantations (EU), Grassland (GL), Wetland (WT), Settlements (SM) and Young Sugarcane (YS). The Red band on other hand played a pivotal role in the classification of Indigenous Forest (IF) and *Pinus* tree plantations (PS) whereas Green wavelengths aided in classifying Bare Soil (BS) as well as Mature Sugarcane (MS). The SWIR region of the spectrum helped significantly in the classification of water bodies i.e. River (RV) and Ocean (OC).

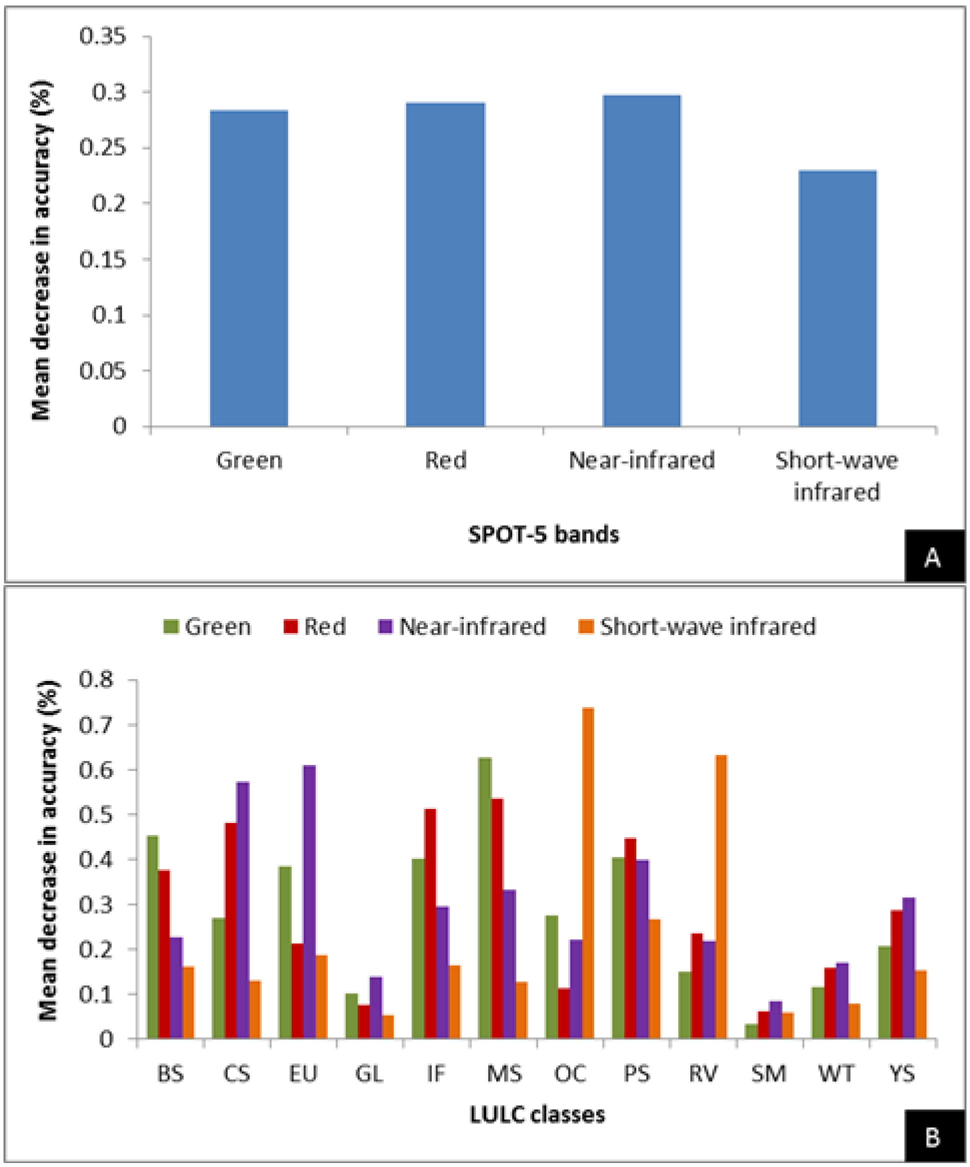


**Figure 2**. The importance of SPOT-5 bands in LULC classification; for the entire LULC classes (A) and for each individual LULC class (B). The highest mean decrease in accuracy indicates the most important band. The classes are: BS (Bare soil), CS (Coastal sand), EU (*Eucalyptus grandis* plantation), GL (Grassland), IF (Indigenous forest), MS (Mature sugarcane), OC (Ocean), PS (*Pinus* tree plantation), RV (River), SM (Settlements), WT (Wetland), and YS (Young sugarcane).

### 2.4.3. Visual comparison of classification maps

Classified data often manifest a “salt-and pepper” appearance as a result of the inherent spectral variability encountered by a classifier when applied on a pixel-by-pixel basis. In such situations it is important to smooth the classified output to show only the dominant classification (Lillesand *et al.*, 2008). In that regard, post classification smoothing was applied to the classified images so as to eliminate isolated pixels and generate a less noisy image (Al-Ahmadi and Hames, 2008). A majority filter ($5 \times 5$ kernel) was applied to the two images as proposed by Lillesand *et al.* (2008) and the results were then analyzed. The results (Figure 3) showed that both classifiers performed relatively well in classifying some of the broader cover types such as Indigenous Forest, Grassland, and Bare Soil. However, there were minor problems encountered in mapping other broad cover types such as *Eucalyptus grandis* and *Pinus* tree plantations, Mature and Young Sugarcane, as well as River and Ocean. Specifically, some sections of the *Eucalyptus grandis* plantations were frequently misclassified as *Pinus* tree plantation. Conversely, there were sections of the *Pinus* tree plantations misclassified as *Eucalyptus grandis* plantation. In addition, both algorithms found it difficult to discriminate between Young Sugarcane and Mature Sugarcane. Small sections of the river were incorrectly classified as ocean and there were also parts of the ocean misclassified as river. Classes that cover relatively smaller spatial extents such as Settlements and Wetland were not mapped as accurately as the broader LULC classes.

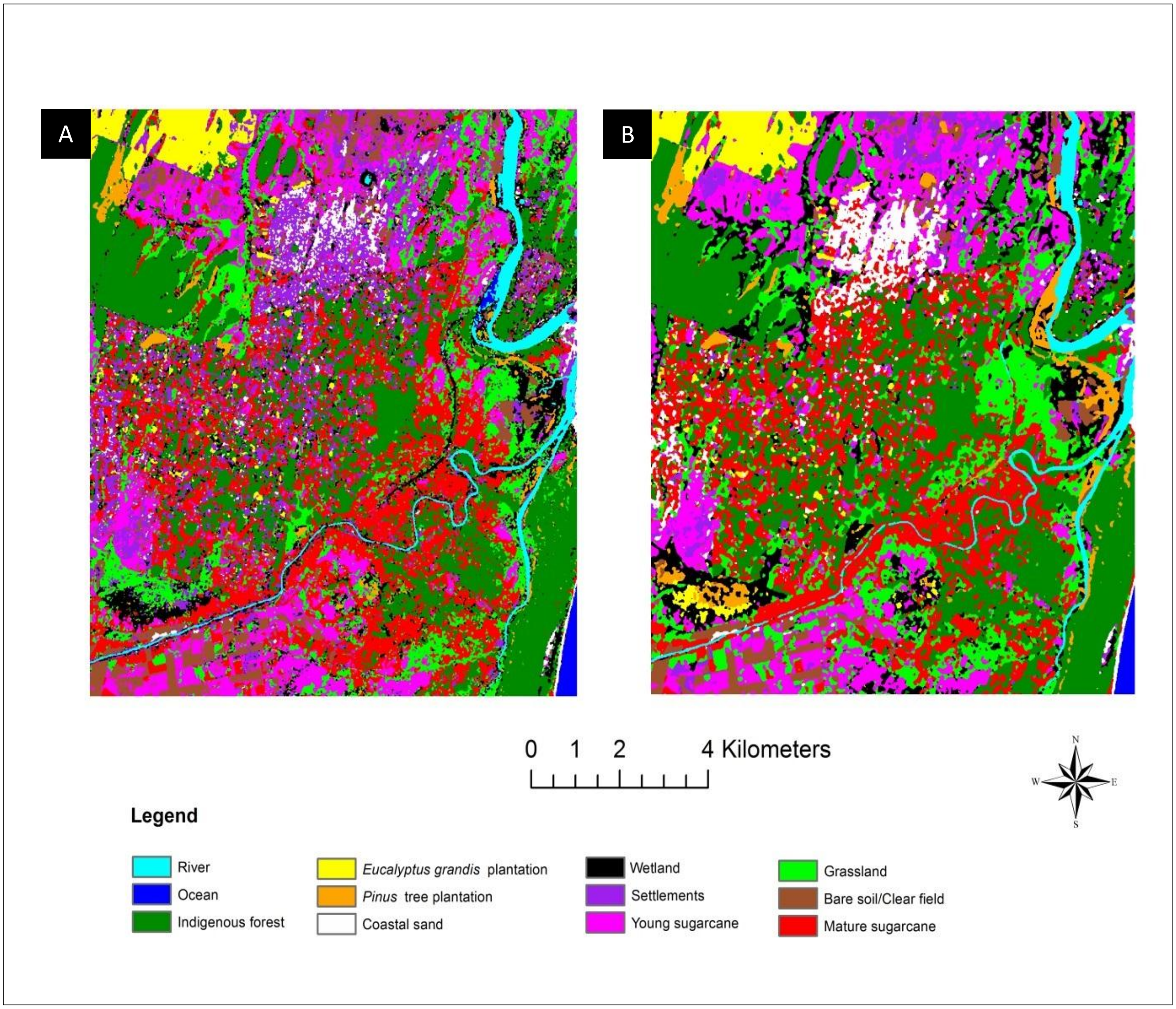


**Figure 3**. Classification maps generated by Random Forests (A) and Maximum Likelihood (B) classifiers. Map A was generated using EnMap Box *image*RF while Map B was computed using ENVI 4.7 image processing software.

### 2.4.4. Accuracy assessment

Tables 1 and 2 contain detailed information on the confusion matrices computed for both ML and RF classifiers. The overall accuracies from the two tables indicate that the advanced RF algorithm outperformed the ML classifier. RF achieved an overall accuracy of 80.2% whereas ML attained an overall accuracy of 65.1%. For both classifiers however, user's and producer's accuracy values for Bare Soil, Grassland and Indigenous Forest were relatively high. Precisely, both user's and producer's accuracy values ranged between 80 and 89% for ML, and between 90 and 93% for RF. However, there was a slight decline in accuracy when the same values were assessed for the finer LULC classes such as *Eucalyptus grandis* plantation (EU) and *Pinus* tree plantation (PS), Mature Sugarcane (MS) and Young Sugarcane (YS), as well as Ocean (OC) and River (RV). Both user's and producer's values for the six classes ranged between 69 and 86% for RF, while the same values were significantly lower for ML as they ranged between 54 and 77%. Settlements (SM) and Wetlands (WT) produced the worst performance amongst the 12 LULC classes considered in this study. The two classes failed to achieve a single value above the 68% mark.

**Table 1.** Confusion matrix and associated Random Forest accuracies based on the 30% independent test dataset. The accuracies include: Overall accuracy (OA), user's accuracy (UA) and producer's accuracy (PA).

| | BS | CS | EU | GL | IF | MS | OC | PS | RV | SM | WT | YS | **Row total** | **UA (%)** |
|---|---|---|---|---|---|---|---|---|---|---|---|---|---|---|
| BS | 30 | 0 | 0 | 0 | 0 | 0 | 0 | 0 | 0 | 0 | 2 | 0 | 32 | 93.75 |
| CS | 3 | 18 | 0 | 0 | 0 | 0 | 0 | 0 | 0 | 5 | 0 | 0 | 26 | 69.23 |
| EU | 0 | 0 | 20 | 0 | 0 | 0 | 0 | 0 | 0 | 0 | 3 | 0 | 23 | 86.96 |
| GL | 0 | 1 | 0 | 28 | 0 | 0 | 0 | 0 | 0 | 1 | 0 | 0 | 30 | 93.33 |
| IF | 0 | 0 | 1 | 0 | 29 | 0 | 0 | 1 | 0 | 0 | 0 | 0 | 31 | 93.55 |
| MS | 0 | 0 | 4 | 0 | 0 | 20 | 0 | 0 | 1 | 0 | 0 | 0 | 25 | 80 |
| OC | 0 | 2 | 0 | 0 | 0 | 0 | 23 | 0 | 3 | 0 | 0 | 0 | 28 | 82.14 |
| PS | 0 | 0 | 0 | 0 | 1 | 4 | 0 | 22 | 0 | 2 | 1 | 0 | 30 | 73.33 |
| RV | 0 | 0 | 0 | 0 | 0 | 0 | 4 | 0 | 22 | 1 | 0 | 2 | 29 | 75.86 |
| SM | 0 | 3 | 1 | 0 | 0 | 1 | 0 | 0 | 0 | 13 | 3 | 1 | 22 | 59..09 |
| WT | 0 | 0 | 0 | 3 | 0 | 0 | 0 | 0 | 0 | 2 | 17 | 3 | 25 | 68 |
| YS | 0 | 0 | 0 | 0 | 0 | 0 | 0 | 3 | 0 | 1 | 3 | 16 | 23 | 69 |
| **Column total** | 33 | 24 | 26 | 31 | 30 | 25 | 27 | 26 | 26 | 25 | 29 | 22 | 324 | |
| **PA (%)** | 90.91 | 75 | 76.92 | 90.32 | 96.67 | 80 | 85.19 | 84.62 | 84.62 | 52 | 58.62 | 72.73 | | |
| **OA (%)** | 80.2 | | | | | | | | | | | | | |

**Table 2.** Confusion matrix and associated Maximum Likelihood (ML) accuracies based on the 30% independent test dataset. The accuracies include: Overall accuracy (OA), user's accuracy (UA) and producer's accuracy (PA).

| | BS | CS | EU | GL | IF | MS | OC | PS | RV | SM | WT | YS | **Row total** | **UA (%)** |
|---|---|---|---|---|---|---|---|---|---|---|---|---|---|---|
| BS | 21 | 0 | 0 | 0 | 2 | 0 | 0 | 0 | 0 | 1 | 0 | 0 | 24 | 87.5 |
| CS | 0 | 12 | 0 | 0 | 2 | 0 | 4 | 2 | 0 | 0 | 2 | 0 | 22 | 54.55 |
| EU | 0 | 0 | 17 | 0 | 0 | 4 | 0 | 6 | 0 | 0 | 0 | 0 | 27 | 62.96 |
| GL | 0 | 0 | 0 | 26 | 0 | 2 | 0 | 1 | 0 | 0 | 0 | 0 | 29 | 89.66 |
| IF | 0 | 0 | 2 | 1 | 32 | 0 | 4 | 0 | 0 | 1 | 0 | 0 | 40 | 80 |
| MS | 2 | 0 | 0 | 0 | 0 | 25 | 0 | 1 | 7 | 1 | 0 | 0 | 36 | 69.96 |
| OC | 0 | 0 | 4 | 0 | 0 | 0 | 8 | 0 | 0 | 0 | 5 | 0 | 17 | 47.05 |
| PS | 0 | 0 | 4 | 0 | 0 | 2 | 0 | 16 | 3 | 0 | 0 | 2 | 27 | 59.26 |
| RV | 2 | 2 | 0 | 0 | 0 | 0 | 0 | 0 | 18 | 0 | 8 | 0 | 30 | 60 |
| SM | 0 | 8 | 0 | 0 | 0 | 0 | 0 | 0 | 0 | 4 | 0 | 1 | 13 | 30.77 |
| WT | 0 | 0 | 0 | 2 | 0 | 0 | 0 | 2 | 0 | 3 | 12 | 4 | 24 | 54.17 |
| YS | 0 | 0 | 0 | 0 | 0 | 9 | 0 | 0 | 2 | 1 | 0 | 24 | | 66.67 |
| **Column total** | 25 | 22 | 27 | 29 | 36 | 42 | 16 | 28 | 30 | 11 | 27 | 31 | 324 | |
| **PA (%)** | 84 | 54.55 | 62.96 | 89.66 | 88.89 | 59.52 | 50 | 57.14 | 60 | 36.36 | 44.44 | 77.41 | | |
| **OA** | 66.1 | | | | | | | | | | | | | |

Table 3 contains information of the performance of the Kappa and Total disagreement measures of accuracy assessment. Total disagreement is the sum of Quantity disagreement and Allocation disagreement values. Results indicated that Kappa disagreement values for ML and RF were 37% and 22% respectively. Total disagreement values on the other hand were lower for both classifiers. Precisely, the Total disagreement for ML was 34% whereas the Total disagreement for RF was 21%. The lower Total disagreement suggests that the Kappa index reports more error than is actually present in the classification (Adelabu *et al.*, In press).

**Table 3.** Comparison of Kappa and Total disagreement methods of classification assessments. All calculations were done using the confusion matrix proposed by Pontius Jr and Millones (2011) available from www.clarku.edu/~rpontius.

| **Parameters** | **ML** | **RF** |
|---|---|---|
| Kappa | 0.63 | 0.78 |
| Kappa disagreement (%) | 37 | 22 |
| Allocation disagreement (%) | 30 | 17 |
| Quantity disagreement (%) | 4 | 4 |
| Total disagreement (%) | 34 | 21 |

### 2.4.5. Statistical significance of classification results

In this study, the McNemar test was utilized for testing the statistical significance and superiority of one algorithm over the other. Of the total pixels (n =324) compared for the accuracy assessment, 256 were correctly classified by both classifiers, whereas 34 were misclassified by both algorithms. On other hand, 20 pixels were correctly classified by RF (classifier 1) but not by MLC (classifier 2) and 14 pixels were correctly classified by ML but not by RF. The McNemar test thus yielded a $Z$ value of 2.45 at 5% level of significance. Since the value of $Z$ was greater than 1.96, the difference in accuracy between the two classifiers was considered to be statistically significant, and a conclusion was reached that the RF algorithm is superior to the conventional ML classifier.

## 2.5 Discussion

In the last three decades, coarse resolution multispectral sensors such as Landsat have been used extensively for the classification of Earth surface features. However, LULC maps derived from such datasets are often regarded as inadequate in quality if based on traditional statistical classifiers. The problem with conventional statistical classifiers is that they assume members of all class data are normally distributed, which is not true for remote-sensing images (Song *et al.*, 2012). With the advent of advanced machine learning classifiers, the use of traditional per-pixel classifiers has gradually decreased and high classification accuracy can be achieved. In addition, advanced machine learning algorithms have been shown to increase classification accuracy in coarse resolution datasets (Duro *et al.*, 2012; Dixon and Candade, 2008; Na *et al.*, 2009). In this study, SPOT-5 (10 m) data was used to classify LULC in St Lucia, KwaZulu-Natal using the RF ensemble algorithm. The performance of the RF classifier was then compared to that of the well-known ML algorithm as this classifier is often used as the baseline for comparing machine learning classifiers (Wulder and Franklin, 2003). The study also aimed to bridge the gap between previous studies by breaking down broader Level I classes (Commercial forest plantations and Sugarcane fields) into finer Level II classes (*Eucalyptus grandis* plantation and *Pinus* tree plantation; as well as Mature Sugarcane and Young Sugarcane).

The study has shown that the use of SPOT-5 imagery in conjunction with RF significantly improves the accuracy of LULC maps when compared to the traditional ML method. The RF based classifier achieved an overall accuracy of 80.2% compared to 66.1% for the ML method. The results were found to be consistent with those of Na *et al.* (2009), and also Waske and Braun (2009), as they clearly demonstrated the superiority of RF over ML. The superior nature of RF can be attributed to its non-parametric approach which helps avoid some of the problems encountered by conventional statistical classifiers (Pal, 2005; Rodríguez-Galiano *et al.*, 2012b). RF has no distributional assumptions on the input data and does not suffer from overfitting nor a long training time (Watts and Lawrence, 2008; Watts *et al.*, 2009). Moreover, RF is easy to use and requires only two parameters (*ntree* and *mtry*) to be defined. Previous studies have shown that the default value of *mtry*, defined as the square root of input variables, results in low OOB error (Mansour *et al.*, 2012; Adam *et al.*, 2012). Similar conclusions were drawn in this study as the default value of *mtry* (n = 2 in this case) repeatedly produced low OOB error with all *ntree* values.

Furthermore, using the RF algorithm, the study was able to provide an insight into the importance of each of the SPOT-5 bands in the landscape classification process. Results indicated that the near-infrared band was the most instrumental variable in discriminating between the different LULC classes considered in this study. The dominance of this band can be explained by the fact that wavelengths from this region help in discriminating between various surface cover types such as plant species, soil types and water bodies, which were all present in the study area (Lillesand *et al.*, 2008). Interestingly, the shortwave-infrared band was the least important variable in the classification. This band is useful in detecting moisture and effectively separating water bodies (Duro *et al.*, 2012), and thus did not have a major role to play in the classification as only 2 of the 12 LULC classes were water bodies (River and Ocean). In addition, the shortwave-infrared band has a spatial resolution of 20 m (Lillesand *et al.*, 2008), and is unable to detect ground surface objects less than 20 m in size.

Using EnMap Box *(imageRF*), as well as ENVI 4.7 image processing software, classification maps were generated for both RF and ML classifiers respectively. Generally, both classifications showed a relatively accurate depiction of the larger LULC categories in the study area. Particularly, the classifiers were efficient in the mapping of three classes (Indigenous Forest, Grassland and Bare Soil). The large spatial extent of the classes resulted in the good performance of algorithms as homogenous areas for collecting training samples were relatively abundant and easy to identify. For the smaller LULC classes however, there was a remarkable reduction in classification performance mainly due to the following factors. Firstly, the dataset used in this study had a relatively coarse spatial resolution (10m) and thus suffered from the mixed pixel problem (Lu and Weng, 2007). Secondly, homogenous areas for collecting training samples are difficult to spot in coarse resolution data, especially when dealing with LULC classes that cover relatively small spatial extents (Foody and Mathur, 2004b).

Generally, both classifiers seemed to experience difficulties in discriminating between classes with similar spectral profiles. These classes were *Eucalyptus grandis* plantation and *Pinus* tree plantation, Mature Sugarcane and Young Sugarcane, as well as River and Ocean. To counteract this problem, an alternative approach would be to use multispectral data with both higher spatial and spectral resolution such as WorldView-2. Overall, the results of this study indicate that SPOT-5 (10 m) data can be successfully used for mapping broad LULC classes.

## 2.6 Conclusion

The present study used SPOT-5 data and the RF ensemble algorithm to classify LULC in a complex environment consisting of diverse LULC categories and the following conclusions were reached:

- SPOT-5 (10 m) multispectral data has the potential to discriminate broad LULC categories in heterogeneous ecosystems using the RF algorithm.
- However, finer LULC classes such as *Eucalyptus grandis* plantation and *Pinus* tree plantations can often be difficult to separate using moderate resolution SPOT-5 data due to the mixed pixel problem.
- When compared to the conventional ML method, the RF algorithm produces better results and can identify optimal wavelengths for classifying specific LULC types.
- SPOT-5 data remains a powerful tool for LULC classification so long as advanced machine learning classifiers are used.

The next section will therefore assess whether WorldView-2 multispectral data with its improved spatial (2m) and spectral resolutions (8 bands) could be used to resolve the problems encountered by traditional coarse resolution datasets in small-scale LULC mapping.

# CHAPTER 3

# Discriminating spectrally similar land use/cover classes using WorldView-2 imagery in KwaZulu-Natal, South Africa

## 3.1 Abstract

Multispectral image data has been applied in land use/cover (LULC) classification with varying results. Problems are encountered when separating features with subtle differences such as species or age. WorldView-2 multispectral data, with strategically positioned bands, was used to discriminate amongst three sets of spectrally similar LULC classes near St Lucia (KwaZulu-Natal) using the advanced Random Forest (RF) algorithm. Results from the accuracy assessment indicated that WorldView-2 imagery in conjunction with RF can be used to differentiate between LULC categories exhibiting similar spectral properties as the classification yielded an overall accuracy of 91.23%. Furthermore, RF variable importance measures provided insight into wavelengths most influential in the classification process. Overall, the study demonstrated the utility and robustness of WorldView-2 image data in classifying LULC features at fine spatial scales, which enables effective and efficient applications for land use planning and management.

**Keywords:** WorldView-2; discrimination; spectrally similar classes; Random Forest

## 3.2 Introduction

Over the years, a number of studies have sought to discriminate spectrally similar ground-cover objects such as soil types (Metternicht and Zinck, 1997; Brown *et al.*, 1999), forest tree species (Van Aardt, 2000), and crop varieties (Daughtry, 2001). Generally, the studies have used various approaches ranging from field-work based methods (Jia *et al.*, 2011), to sophisticated laboratory based techniques (Song *et al.*, 2011). Recently however, research on spectral discrimination has focused on the use of remote sensing as a tool to effectively separate land use/cover (LULC) classes exhibiting similar spectral responses (Pugh and Waxman, 2006). Compared to conventional methods, remote sensing is cost-effective, less-time-consuming and reduces intensive field sampling and laboratory analysis (Adam *et al.*, 2012). Multispectral sensors such as Landsat and SPOT cover vast areas of land at frequent intervals, making remote sensing an ideal alternative to conventional methods. However, traditional multispectral sensors (Landsat and SPOT ) are limited by coarse spatial resolution and are therefore unable to adequately differentiate between objects smaller than the sensor’s coarse ground resolution (Immitzer *et al.*, 2012; Moran, 2010).

The development of high resolution multispectral sensors such as Ikonos provides unique opportunities for those seeking to classify LULC into finer levels of detail (Mansour *et al.*, 2012). Due to technological limitations however, the sensors have been limited to providing imagery comprising only four spectral bands, making the distinction of LULC classes of similar coloration difficult (Zhou *et al.*, 2012). To tackle this problem, researchers have recommended the use of hyperspectral data as these contain hundreds of observation channels with the capability to discern subtle variations in ground-cover objects (Melgani and Bruzzone, 2004). Nonetheless, the use of hyperspectral image data carries its own limitations regarding cost, accessibility, processing and high dimensionality (Mutanga *et al.*, 2012). With the availability of the WorldView-2 satellite, multispectral remote sensing has been transformed remarkably and limitations pertaining to coarse spatial and spectral resolution are now a thing of the past. (Novack *et al.*, 2011; Peerbhay *et al.*, In press). In addition to the four traditional bands (Blue, Green, Red and Near-infrared 1), WorldView-2 contains four new bands (Red edge, Yellow, Coastal blue and Near-infrared 2) that were previously unavailable in conventional high resolution multispectral sensors  (Marchisio *et al.*, 2010; Zengeya *et al.*, 2012).

The additional four bands are expected to offer an improvement of up to 30% in  accuracy, when compared to classifications conducted with only the four conventional bands available in sensors such as GeoEye-1 or Ikonos (Zhou *et al.*, 2012). In an urban context, Novack *et al.* (2011) has already shown that the use of these bands significantly improves classification results relative to classifications performed using only the four traditional bands offered by the Quickbird-2 sensor. Moreover, the study showed that targets with similar spectral responses such as ceramic tile roofs and bare soil, as well as asphalt and dark asbestos roofs can be easily separated when the additional bands of WorldView-2 were employed using the object-based classification procedure. However, this study was conducted in an urban setting, making its results inapplicable to all landscapes. The question therefore remains whether the new bands in the WorldVeiw-2 sensor could help improve discrimination amongst spectrally similar classes that are not commonly found in urban areas such as *Eucalyptus grandis* and *Pinus* tree plantations; mature sugarcane and young sugarcane, as well as water from the river and ocean (Figure 1).

Numerous classifiers have been developed for the classification of remotely sensed imagery, with varying degrees of success (DeFries and Chan, 2000; Huang *et al.*, 2002). Amongst these classifiers, the maximum likelihood and minimum distance algorithms have been the most widely used (Ghose *et al.*, 2010; Kavzoglu and Mather, 2003). Popularity of the two algorithms can be attributed to their simplicity and availability in most software packages, as well as their ability to generate acceptable results (Lu and Weng, 2005; Song *et al.*, 2012). Both these classifiers, however,  have their constraints in relation to distributional assumptions and restrictions on the input data types (Kavzoglu, 2009; Kavzoglu and Mather, 2003). Scientists and practitioners have therefore made great efforts in developing advanced classification techniques in an effort to overcome the shortfalls of traditional statistical classifiers, and produce improved classification performance (Kavzoglu, 2009; Lu and Weng, 2007). Examples include expert systems, neural networks, decision trees and support vector machines (Friedl and Brodley, 1997; Kavzoglu, 2009; Lu and Weng, 2007). More recently, attention has been focused on the use of the Random Forest (RF) algorithm for solving problems associated with the classification of remotely sensed imagery (Rodríguez-Galiano *et al.*, 2012b).

Random Forest is an ensemble algorithm developed in the field of machine learning that uses a decision tree as the base classifier (Chan and Paelinckx, 2008b). This algorithm is relatively unknown and has not been explored exhaustively in the remote sensing community (Watts *et al.*, 2009). Some studies suggest that RF is unexcelled in accuracy among current algorithms (Lawrence *et al.*, 2006; Watts and Lawrence, 2008). As a result, there has been a marked increase in the number of studies employing RF for remote sensing image classification (Stumpf and Kerle, 2011; Peters *et al.*, 2011; Chan *et al.*, 2012). In this study, WorldView-2 multispectral data was used to discriminate amongst three pairs of spectrally similar LULC classes using the advanced RF ensemble algorithm.

| Spectrally similar classes | Sample plots from Worldview-2 image used to compute the spectral profile | | Averaged spectral profiles |
|---|---|---|---|
| *Eucalyptus grandis* (**A)** and *Pinus* tree plantations (**B**) |  A |  B | 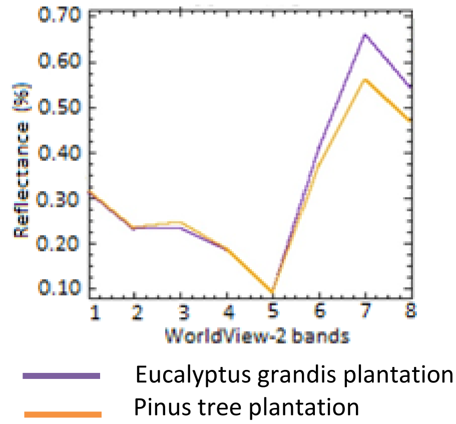  |
| Mature Sugarcane (**A**) and Young Sugarcane (**B**) |  A |  B | 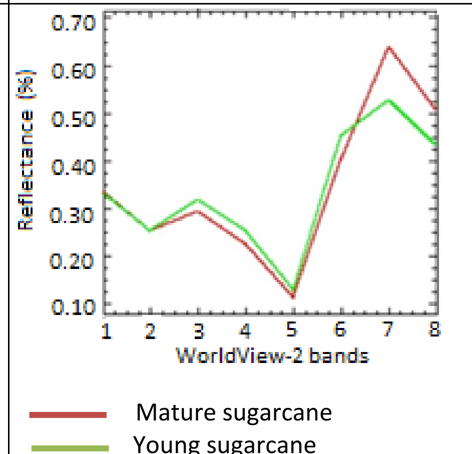  |
| River water( **A**) and Ocean water (**B**) |  A |  B | 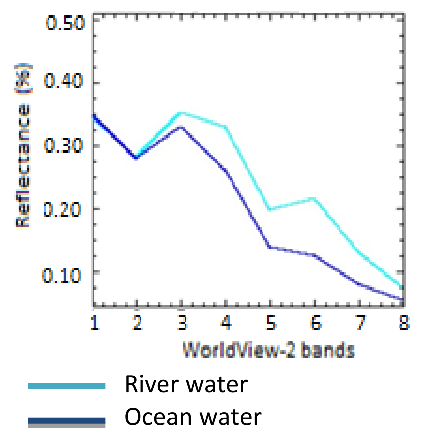  |

**Figure 4**. Three sets of spectrally similar classes assessed in this study, with sample image plots and resultant spectral profiles highlighting challenges presented for discrimination.

## 3.3 Materials and Methods

### 3.3.1 Study area

The study was conducted in a heterogeneous ecosystem located near the small town of St Lucia, KwaZulu-Natal (refer to Figure 1). The site covers an area of approximately 136 $km^2$ and extends from 32°18'43.805" to 32°25'25.975" E, and from 28°20'39.114" to 28°27'23.095” S. This area is characterized by extensive commercial plantations, sugarcane farms and indigenous forest. The area covers part of the Mfolozi/Msunduzi estuarine system which flows in a south westerly direction as it emerges from the Indian Ocean. Wetlands were once dominant in this ecosystem before agriculture subsequently converted 61% of the wetland system into highly productive sugarcane estates (Vivier *et al.*, 2010). Rainfall ranges from 1200 mm to 1300 mm per annum with approximately 60 % of the rainfall falling in summer (Mafuratidze, 2010).

### 3.3.2 Image acquisition and pre-processing

High resolution multispectral imagery was acquired over the study area using the WorldView-2 sensor on 12 May 2012. The image was acquired during sunny, low wind and clear skies at 12:47 am (GMT) and consisted of 8 multispectral bands with a 2 m spatial resolution. The spectral ranges of the bands were as follows: Coastal blue (400–450 nm), Blue (450–510 nm), Green (510–581 nm), Yellow (585–625 nm), Red (630–690 nm), Red-edge (705–745 nm), Near-infrared 1 (770–895 nm), and Near-infrared 2 (860–1040 nm). Digital numbers (DN) from the image were then converted into top of atmosphere reflectance using the Quick Atmospheric Correction (QUAC) algorithm built into Environment for Visualising Images (ENVI) 4.7 image processing software (ENVI, 2006). This ensures that meaningful spectral reflectance signatures are derived from the image for each of the LULC classes (Immitzer *et al.*, 2012). Thereafter, the image was geometrically corrected using georeferenced aerial photographs (0.5m) based on 20 ground control points that were evenly distributed across the two images (Zengeya *et al.*, 2012). The 1st order polynomial transformation technique was applied, and a Root Mean Square error

(RMSE) of 0.33% of a pixel was achieved. The RMSE obtained from the geo-rectification process was considered sufficient as classes of interest from both images overlapped perfectly (Ozdemir and Karnieli, 2011).

### 3.3.3 Field data collection

Hawth's Analysis Tools (HAT) in ArcGIS 9.3 software was used to generate 540 sample points on a LULC map of the study area extracted from the KwaZulu-Natal Provincial LULC (KZNPLULC) map. To ensure that sample points were distributed only over the LULC classes considered in the study, spatial masking was applied to other LULC classes in the map so as to retain only the classes of interest i.e. Commercial forest plantations, Sugarcane fields, and Water bodies. The KZNPLULC map is available for free download from the following website: http://bgis.sanbi.org/kzn/landcover.asp, and was developed in 2006 using SPOT-4 satellite imagery. The points were subsequently stored in a global positioning system (GPS) device and used to locate the field sites. Once the sample site was located in the field, a 10 m × 10 m plot was created to cover a homogenous area of the LULC class and a GPS reading was recorded. Ancillary data was then used to distinguish *Eucalyptus grandis* plantations from *Pinus* tree plantations, as well as young sugarcane fields from mature sugarcane fields. For commercial forest plantations, the ancillary data was in the form of a forest stand map containing species data on all the commercial forest plantations present in the study area. For sugarcane fields however, each field was classified as either mature sugarcane or young sugarcane based on known planting. Additional reference data for locations that could not be accessed due to limiting factors such as rugged terrain was obtained by visually interpreting high resolution aerial photographs (0.5 m) of St Lucia. The HAT extension in ArcGIS 9.3 was then used to randomly split the data (n = 540) into a 70% training (n = 378) and 30% validation (n = 162) dataset. Training data was used to optimize the RF classification and to train the prediction model, whereas the validation data was used to test the quality and reliability of the prediction model (Ismail and Mutanga, 2010). The splitting of the dataset was performed three times to avoid any potential bias that may occur in the selection process.

### 3.3.4 Random Forest (RF)

The Random Forest (RF) algorithm is an ensemble-based technique established by Leo Breiman and Adele Cutler to alleviate the instability of conventional ensemble algorithms (Mansour *et al.*, 2012)**.** RF classifies remote sensing imagery by building a large number of classification and regression trees that are trained on random bootstrapped samples of the calibration data (Sesnie *et al.*, 2010). Each of these trees are built using a new subset from the original training dataset that contains approximately 2/3 of the cases (Rodriguez-Galiano *et al.*, 2012a). The nodes of the trees are then split using the best split variable amongst a subset of randomly nominated variables (Loosvelt *et al.*, 2012). Pixels are then assigned to classes that obtain the greatest number of votes from the ensemble of classification trees (Ghimire *et al.*, 2010). The remaining one-third (1/3) of the training data is included as part of another subset known as the "out-of-bag" (OOB) sample (Rodríguez-Galiano *et al.*, 2012b). The OOB sample is used as a measure of accuracy that produces results comparable to external accuracy assessments, so long as there is no bias in the reference data (Watts *et al.*, 2009). In contrast to conventional statistical methods, RF is not sensitive to background noise, does not over-fit the data distributions, and is capable of handling unbalanced datasets (Walton, 2008). RF is also simple to train because it requires just two input parameters: (1) the number of trees (*ntree*), and (2) the number of input variables (*mtry*) (Dye *et al.*, 2011).

### 3.3.5 Variable importance using the RF algorithm

Variable importance provides an indication of the relative value of predictor variables in the classification (Walton, 2008). Random Forest determines three variable importance measures, (i) the number of times a variable is chosen, (ii) the Gini importance and, (iii) the permutation accuracy importance measure (Adam *et al.*, 2009). The third measure is regarded as the most fundamental owing to its ability to evaluate variable importance through internal OOB estimates while the forests are constructed (Mansour *et al.*, 2012; Adam *et al.*, 2012). Another key advantage of the RF variable importance is that it not only deals with the impact of each variable individually, but also considers multivariate interactions among variables (Dye *et al.*, 2012). In this study, the mean decrease in accuracy (MDA) was used to measure and rank the importance each variable, and thereafter identify the bands which contributed the most in the classification process (Mansour *et al.*, 2012; Adam *et al.*, 2012).

### 3.3.6 Classification accuracy assessment

One of the most common means of expressing accuracy is the preparation of a classification error matrix, otherwise known as a confusion matrix (Lillesand *et al.*, 2008). Literature often suggests that a confusion matrix should be computed using an independent test data set that has not been used in the training phase (Mansour *et al.*, 2012). In that regard, a 30% validation dataset (n = 162) which was set aside from the original dataset (n = 540) was used to assess the prediction performance of the RF based algorithm, while the training data (n = 378) was used to perform the classification. Subsequent to that, three measures were calculated i.e. overall accuracy (OA), user's accuracy (UA), and producer's accuracy (PA). OA is the average of the individual class accuracies, which are usually expressed in percentage (Mather and Koch, 2011). UA expresses the probability that a pixel belongs to a given class and the classifier has labelled the pixel correctly into the same given class (Petropoulos *et al.*, 2012a). PA, on the other hand, indicates the probability that the classifier has correctly labelled an image pixel (Petropoulos *et al.*, 2012b).

The kappa index has established itself as the most commonly used measure of assessing the amount of agreement between the reference data and the classifier used to perform the classification (Foody, 2004). However, recent studies (Pontius Jr and Millones, 2011) have shown that kappa indices are prone to error, and can often give information that is redundant or misleading for practical decision making. For this reason, Pontius Jr and Millones (2011) recommend that researchers abandon the use of kappa indices and replace these indices with a more useful and simpler approach that focuses on two components of disagreement between maps. In this study, quantity disagreement and allocation disagreement measures were used as recommended by the aforementioned authors. Quantity disagreement refers to the amount of pixels of a class from the training data that are different from the quantity of pixels of the same class in the test data. Allocation disagreement, on the other hand, refers to the number of pixels that have a less than optimal spatial allocation in the test data , with respect to the training data (Pontius Jr and Millones, 2011).

## 3.4 Results

### 3.4.1 Tuning of RF parameters

In an effort to determine the optimal RF parameters, *mtry* and *ntree* values were optimized using the grid search method and a 10-fold cross validation. The OOB estimate of error was then used as a measure of assessing the prediction performance of the different parameter combinations. Since the overall dataset (n = 540) was split into three calibration (70%) and validation (30%) datasets, parameters from the three datasets were compared and the one with the lowest OOB error was selected to perform the final classification. In terms of optimising the RF parameters, the best model yielded an OOB error of 8.16%, and was produced by *ntree* values of 3500 and 4500 together with an *mtry* value of 3. However, since two *ntree* values yielded this value (8.16%), the larger *ntree* (4500) was chosen as the optimal *ntree* because literature suggests that a high number of trees results in a more stable model (Adam *et al.*, 2012; Mansour *et al.*, 2012).

### 3.4.2 Variable importance

In this study, the RF variable importance was used as a ranking index to determine the relative value of predictor variables in the classification. Based on the overall variable importance (Figure 3A), the Near-infrared 2 (NIR-2) and Near-infrared 1 (NIR-1) wavelengths played the most important role in the classification of spectrally similar LULC classes considered in this study. Similarly, the Coastal blue band (13.6%) also displayed relatively good performance, consequently yielding the third highest MDA amongst the 8 bands. Other variables that played a notable role in the classification were the Green (11.64%) and Red (11.4%) bands which were ranked fourth and fifth respectively by the RF variable importance algorithm. Interestingly, the new Yellow band (7.7%) was the least important variable in the classification as it yielded the lowest MDA value.

Results regarding the performance of each of the WorldView-2 bands in classifying individual LULC classes (Figure 3B) indicated that the NIR-2 band was crucial in the classification of 3 out of the 6 classes examined in the study. Precisely, the NIR-2 band was helpful in discriminating amongst the two water bodies (river (RV) and ocean (OC)), and also mature sugarcane (MS). The Coastal blue band, on the other hand, played the most important role in the classification of young sugarcane (YS). The significant wavelengths for classifying *Eucalyptus grandis* (EU) and *Pinus* (PS) tree plantations also differed, despite their resemblance in spectral curves. The Green band was relatively useful in the classification of *Eucalyptus grandis* plantations, while the Near-imnfrared-1 (NIR-1) band was influential in classifying *Pinus* tree plantations.

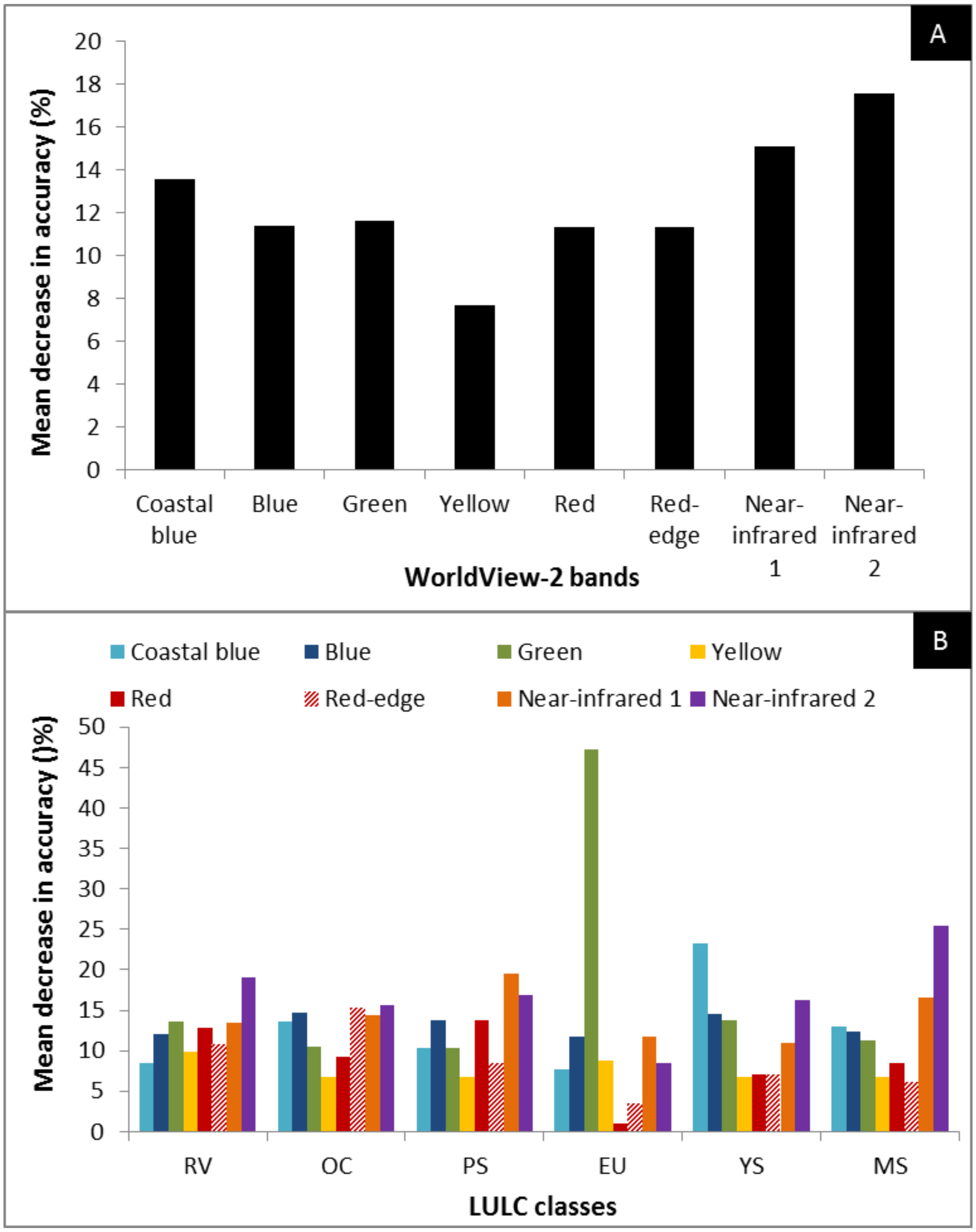


**Figure 5**. The importance of WorldView-2 bands in the classification process; for all six classes considered in this study (A) and for classifying each class individually (B). The highest mean decrease in accuracy indicates the most important band. The spectrally similar classes of interest were: RV (River) versus OC (Ocean); PS (*Pinus* tree plantation) versus EU (*Eucalyptus grandis* plantation); and YS (Young sugarcane) versus MS (Mature sugarcane).

### 3.4.3 Traditional bands versus new bands

Since the WorldView-2 sensor incorporates both traditional (n = 4) and new (n = 4) multispectral bands, the study sought to compare the differences in accuracies obtained using the two different sets of bands. Results indicated that the RF classification performed using the traditional multispectral bands (Blue, Green, Red and NIR-1) yielded an OOB error of 15.84%. On the other hand, the classification performed using only the four new spectral dimensions of WorldView-2 (Red edge, Yellow, Coastal blue and NIR-2) showed an improvement of 5.54% in accuracy as it yielded an OOB error of 10.3%.

### 3.4.4 Accuracy assessment

An accuracy assessment was performed for the RF based classification model using the 30% validation dataset. Based on this validation dataset, a confusion matrix was produced (Table 1). Results showed that the prediction performance of RF was satisfactory as the classification yielded an overall accuracy (OA) of 91.23%. Moreover, both user's accuracy (UA) and producer's accuracy (PA) values were relatively high as only 4 of the 12 observations were less than 90%. Despite the impressive results, there were still minor misclassifications encountered during the classification process. The values in bold in the confusion matrix highlight some of these complications. River (RV) was incorrectly classified as Ocean (OC) once, but Ocean was not incorrectly classified as River. *Eucalyptus grandis* plantation (EU), on the other hand, was misclassified twice as *Pinus* plantation (PS), whereas *Pinus* plantation was not misclassified as *Eucalyptus grandis* plantation. Young Sugarcane (YS) was misclassified once as Mature Sugarcane (MS), while Mature Sugarcane was not misclassified as Young Sugarcane. Interestingly, all classes with the exception of Ocean were misclassified as River once or twice (Table 1).

**Table 1.** Confusion matrix based on the 30% independent test dataset (n = 162 random points). The accuracies include: Overall accuracy (OA), user's accuracy (UA) and producer's accuracy (PA). The spectrally similar classes of interest were: RV (River) versus OC (Ocean); PS (*Pinus* tree plantation) versus EU (*Eucalyptus grandis* plantation); and YS (Young sugarcane) versus MS (Mature sugarcane). Bold values indicate accuracy relevant to the land-classes paired for discrimination.

| | **RV** | **OC** | **EU** | **PS** | **YS** | **MS** | **Row Total** | **UA (%)** |
|---|---|---|---|---|---|---|---|---|
| **RV** | 27 | **1** | 0 | 0 | 0 | 1 | 29 | 93.1 |
| **OC** | **0** | 20 | 0 | 2 | 0 | 0 | 22 | 90.9 |
| **EU** | 1 | 0 | 26 | **2** | 1 | 0 | 30 | 86.67 |
| **PS** | 2 | 0 | **0** | 23 | 0 | 0 | 25 | 92 |
| **YS** | 2 | 0 | 1 | 0 | 25 | **1** | 29 | 86.21 |
| **MS** | 1 | 0 | 0 | 0 | **0** | 26 | 27 | 96.3 |
| **Row total** | 33 | 21 | 27 | 27 | 26 | 28 | 162 | |
| **PA (%)** | 81.82 | 95.24 | 96.3 | 85.19 | 96.15 | 92.86 | | |
| **OA (%)** | 91.23 | | | | | | | |

Kappa and Total disagreement measures of accuracy assessment are presented in Table 2. The Kappa disagreement measure obtained from the classification was 11%, whereas the Total disagreement computed from the allocation and quantity disagreement measures was 9%. The fact that the Total disagreement (9%) is lower than the disagreement from Kappa (11%) suggests that there is less disagreement between the training and test datasets than the traditional Kappa index actually predicts (Adelabu *et al.*, In press).

**Table 2.** Comparison of Kappa and Total disagreement methods of classification assessments. All calculations were done using the confusion matrix proposed by Pontius Jr and Millones (2011) available from www.clarku.edu/~rpontius.

| Parameters | RF |
|---|---|
| Kappa | 0.89 |
| Kappa disagreement (%) | 11 |
| Allocation disagreement (%) | 5 |
| Quantity disagreement (%) | 4 |
| Total disagreement (%) | 9 |

### 3.5 Discussion

In the last decade, there have been numerous remote sensing studies aimed at discriminating LULC classes with similar spectral properties (Dalton *et al.*, 2004; Pugh and Waxman, 2006). Hyperspectral datasets have generally shown great potential in this domain due to the narrow spectral channels that permit an in-depth detection of objects with subtle differences (Chang, 2000; Johnson *et al.*, 2008). More recently, however, multispectral datasets such as WorldView-2 have emerged and attracted a lot of attention owing to the higher spatial (2 m) and spectral properties (8 bands). WorldView-2 provides great potential for distinguishing between spectrally related targets as wavelengths from this sensor are strategically positioned to detect slight variations in Earth surface features (Ozdemir and Karnieli, 2011). In that regard, the present study sought to evaluate the performance of this fairly new WorldView-2 sensor in discriminating spectrally similar LULC classes in St Lucia (KwaZulu-Natal) using the advanced RF algorithm.

Results from the study demonstrated that multispectral data from the WorldView-2 sensor can be successfully used to discriminate amongst spectrally similar LULC objects. Using the advanced RF algorithm, an overall classification accuracy of 91.23% was achieved. These results were found to be comparable to those of Peerbhay *et al.* (In press) who used WorldView-2 data to classify six spectrally related commercial forest species in KwaZulu-Natal (South Africa) and attained an overall accuracy of 85.23%. The key behind the powerful discrimination ability of WorldView-2 lies in the sharper wavelength channels that are coupled with finer spatial resolution (Immitzer *et al.*, 2012). The two attributes provide the potential for more robust modelling and discrimination of spectral signatures, resulting in more accurate extraction of Earth surface resources (Pacifici, 2011). Furthermore, WorldView-2 has the added advantage of four additional bands that are currently unavailable in other multispectral sensors. These new spectral dimensions target coastal and vegetation LULC types with applications in plant species identification, mapping of vegetation stress, crop types, wetlands, coast water quality and bathymetry (Marchisio *et al.*, 2010). An improvement of 5.54% in classification accuracy was observed when LULC classes were discriminated using only the four new bands in contrast to the conventional wavelengths. Similar conclusions were drawn by Novack *et al.* (2011) who noted an improvement in classification accuracy when the new WorldView-2 bands were used in the classification of urban surfaces.

The study also sought to determine the predictive power of each of the WorldView-2 bands in the landscape classification process. Using the RF variable importance, important wavelengths for discriminating spectrally similar LULC classes in the study area were effectively explored and identified. Results suggested that the near-infrared wavelengths (Near-infrared 1 and Near-infrared 2) were the most instrumental bands in the classification. Immitzer *et al.* (2012), also recognized the significance of the near-infrared region in the classification of ground-cover objects. This region of the spectrum provides more discriminatory power for vegetation analysis and biomass studies, while it effectively separates water bodies from vegetation and also discriminates between soil types (Navulur, 2009). The Coastal blue band, on the other hand, has been proven to be useful for accurately classifying water bodies (Puetz *et al.*, 2009). Interestingly, this band was less instrumental in the classification of water bodies (river and ocean) in the study area. Instead, it played a significant role in the classification of young sugarcane due to the fact that wavelengths from this band are strongly absorbed by plants in the early developmental stages (Navulur, 2009). Several studies have reported that the addition of the Yellow band fills important gaps in the spectrum that relate to our ability to capture vegetation (Marchisio *et al.*, 2010). Despite this ability, the Yellow band was ranked as the least important variable in the classification of features considered in this study. This could be due to the fact that the band is used to identify "yellow-ness" characteristics of targets (Immitzer *et al.*, 2012). Since the commercial forest plantations sampled in this study were healthy and well maintained, the band showed a slight decline in performance.

Overall, the results from this study are a significant contribution towards the use of multispectral data for the discrimination of spectrally similar LULC objects. The high classification accuracy suggests that WorldView-2 is a reliable and cost-effective alternative to time consuming methods such as land surveying. However, the interpretation of these results can only be regarded as preliminary, since further research is needed to widen the use of WorldView-2 imagery in classifying other types of LULC such as soils and other non-vegetative features.

## 3.6 Conclusion

This study used WorldView-2 satellite imagery to separate three pairs of spectrally similar LULC classes in St Lucia (KwaZulu-Natal) and the following conclusions were drawn:

- Multispectral data from the WorldView-2 sensor has great potential to discriminate spectrally similar LULC types in a vegetation dominated environment.
- Using the advanced RF algorithm, an overall classification accuracy of 91.23% was obtained clearly demonstrating the remarkable performance of RF in LULC classification.
- The new near-infrared band (Band 8) was found to be the most instrumental band in the classification of LULC classes considered in this study.
- Overall, the combination of high resolution multispectral data with the RF algorithm is an efficient method for separating classes that exhibit similar spectral responses.

# CHAPTER FOUR

# CONCLUSION

## 4.1 Introduction

Accurate land use/land cover (LULC) information is important for ecological, environmental and socio-economic applications (Li and Shao, 2012). Before satellite imagery became freely available, aerial photography was commonly used to acquire such information (Comber *et al.*, 2004). Although this method produces accurate results, it is costly, time-consuming and labor-intensive. Remote sensing offers a cost-effective and quicker alternative to conventional methods and also covers larger areas at frequent intervals (Petropoulos *et al.*, 2012a; Dixon and Candade, 2008). The aim of this study was to assess the utility of multispectral remote sensing data and the Random Forest (RF) algorithm to reliably map LULC in a heterogeneous environment. The specific objectives were (i) to examine the utility of moderate resolution SPOT-5 data to classify LULC in an ecosystem consisting of diverse LULC categories, (ii) to evaluate the efficiency of high resolution WorldView-2 imagery in the classification of spectrally similar LULC classes, (iii) to rank the importance of SPOT-5 and WorldView-2 bands in the classification of the LULC categories considered in the study.

## 4.2 Examining the utility of moderate resolution SPOT-5 data to classify LULC in an ecosystem consisting of diverse LULC categories

Results from the study demonstrated that moderate resolution SPOT-5 data can be used to discriminate amongst broad LULC categories using both the ML and RF algorithms. However, LULC classes with subtle differences such as *Eucalyptus grandis* and *Pinus* tree plantations; young sugarcane and mature sugarcane; and water bodies from the river and ocean could not be adequately differentiated. In addition, ground-cover objects that covered relatively small spatial extents such as settlements could not be mapped as accurately as the broader LULC categories.

The moderate resolution (10 m) of SPOT-5 data was seen as the underlying factor leading to the above mentioned misclassifications. Moderate resolution datasets are extremely susceptible to the mixed pixel phenomenon which impacts negatively on the generalization ability of image classifiers (Moran, 2010). Consequently, these classifiers encounter difficulties in classifying such datasets when compared to more sophisticated methods such as RF. Results from the study showed that the advanced RF classifier produced results that were significantly better than those obtained through the use of the conventional ML method. Specifically, RF yielded an overall accuracy of 80.2% which was 14.1% better than that of the regularly used ML (66.1%) method. Similar conclusions were drawn by Ok *et al.* (2012) who also used SPOT-5 imagery, however, for the classification of agricultural crop species. In another study, Waske and Braun (2009) obtained comparable results with non-optical Synthetic Aperture Radar (SAR) data. The unprecedented ability of RF can be explained by its non-parametric approach to classification, while the failure of ML to outperform RF can be attributed to its parametric approach to the classification process.

Parametric methods assume that image data are normally distributed, and the statistics computed from the calibration data are representative of all class members (Lu and Weng, 2007). Although this hypothesis is valid to some extent, it may be inaccurate for discriminating LULC categories that consist of several sub-classes, as is the case in complex ecosysytems (Kavzoglu and Colkesen, 2009). The non-parametric approach of RF, on the other hand, provides alternaitive ways of  producing land cover maps that are potentially robust to differences in brightness values caused by landscape heterogenity, uneven slopes, or high intra-class variability (Ghimire *et al.*, 2010). The approach helps avoid some of the problems encountered by ealier statistical methods as it has no prior assumptions on the input data (Song *et al.*, 2012; Kavzoglu and Mather, 2003). RF also minimises the effect of bias, variance, and instability which usually occurs in other ensembles and single classification and regression trees because the large number of trees are computed from random subsets of the calibration dataset (Mansour *et al.*, 2012; Ismail and Mutanga, 2010).

In addition, RF is faster in training when compared to ensemble methods and needs only two parameters to be specied i.e. the number of trees in the forest (*ntree*) and the number of variables to split the nodes of individual trees (*mtry*) (Dye *et al.*, 2011). Lastly, one of the most attractive properties of RF is that it can detect outliers which is useful when looking at classes that have been mislabelled (Peters *et al.*, 2007; Walton, 2008)

### 4.3 Evaluating the efficiency of high resolution WorldView-2 imagery in the classification of spectrally similar LULC classes

WorldView-2, the first ever commercial satellite to carry a high resolution 8-band multispectral sensor was used in an attempt to separate LULC classes that exhibited similar spectral responses. These LULC classes were: *Eucalyptus grandis* and *Pinus* tree plantations; mature sugarcane and young sugarcane; as well as water from the river and ocean. Attempts to separate these LULC classes using moderate resolution SPOT-5 data were unsuccessful. WorldView-2, on the other hand, with its greater spatial (2 m) and spectral resolutions (8 bands), provided greater potential for the discrimination of such LULC features. Results from the study revealed that WorldView-2 data is an effective data source for differentiating among LULC objects exhibiting similar spectral properties. Using the RF based algorithm and the entire WorldView-2 bands; an overall classification accuracy of 91.23% was obtained. This demonstrated the power that the higher spatial and spectral properties of WorldView-2 bring to the classification process.

WorldView-2 is unique from other high resolution multispectral sensors in that it contains four new bands (Coastal blue, Yellow, Red-edge and Near-infrared 2 (NIR-2)) that no other high resolution multispectral sensor possesses. These distinctive wavelengths give remote sensing experts access to spectral domains where discernible variations occur among Earth surface features that may not be picked up by conventional multispectral sensors (Wolf, 2010). When the four new bands were used for the classification process, a relatively low out-of-bag (OOB) error of 10.3% (equivalent to 89.7% overall accuracy) was achieved. In contrast, when only the traditional bands (Blue, Green, Red and NIR-1) were used for the classification, the OOB error increased by 5.54% from 10.3% to 15.54% (equivalent to 84.46% overall accuracy).

Previous studies have shown that the sharper multispectral channels provide greater potential for accurate modeling and discrimination of spectral signatures (Pacifici, 2011). These bands are strategically positioned to unique positions of the electromagnetic spectrum that permit optimum discrimination amongst land surface objects (Mutanga *et al.*, 2012). For instance, the Coastal blue band captures wavelengths shorter than the standard Blue wavelengths and assists in mapping aquatic vegetation or bathymetric studies, due to its ability to penetrate water better than longer wavelengths (Zhou *et al.*, 2012; Navulur, 2009). The red-edge band, on the other hand, is tuned to the region between the Red and NIR wavelengths and provides very sensitive measurements of vegetation types, plant condition, as well as biomass (Mutanga *et al.*, 2012). Wavelengths from the Yellow band are designed to aid in the mapping of senescent vegetation whereas the additional NIR band (NIR-2) is less sensitive to atmospheric conditions and assists in vegetation mapping (Navulur, 2009).

### 4.4 Ranking the importance of SPOT-5 and WorldView-2 bands in the classification of the LULC categories considered in the study

A very important feature of RF is its ability to determine variable importance. Variable importance measures allow the user to determine wavelengths that played a pivotal role in the classification process. The RF algorithm determines the prominence of each predictive variable through assessing changes in mean decrease in accuracy (MDA) values when OOB data for that variable are permuted while all other variables are left unchanged (Peters *et al.*, 2007). It then ranks the variables according to importance, with the most important variable in the classification yielding the highest MDA value. Results from the study suggested that the NIR region of the spectrum played the most significant role in the classification of the LULC classes considered in the study (Chapters 2 and 3). Specifically, when moderate resolution SPOT-5 data were used for the classification of all 12 LULC categories present in the study area (Chapter 2), variable importance measures indicated that SPOT-5's NIR band was the most crucial band in the classification. Similarly, when high resolution WorldView-2 imagery was used for the discrimination of spectrally related targets (Chapter 3), RF variable importance measures ranked the NIR-2 and NIR-1 bands first and second respectively in terms of importance.

However, although the most important wavelengths in the classification from both SPOT-5 and WorldView-2 datasets were identical, the bands that contributed the least towards the classification differed. Results demonstrated that the shortwave-infrared (SWIR) band was the least important SPOT-5 band in the classification, whereas WorldView-2's Yellow band produced the worst performance in the classification of spectrally related targets. More so, wavelengths most instrumental in the classification of *Eucalyptus* grandis and *Pinus* tree plantations, as well as mature sugarcane and young sugarcane differed using both SPOT-5 and WorldView-2 imagery. However, this was not the case for water bodies from the river and ocean as the NIR region of the electromagnetic spectrum played a pivotal role in the classification of these features using both WorldView-2 and SPOT-5 imagery.

### 4.5 Recommendations for future research

Several recommendations for future research are listed below:

- Future research should be focused on the use of multispectral sensors that possess both high spatial and spectral resolution for accurate LULC classification. Higher spatial resolution reduces the mixed pixel problem commonly found in conventional multispectral datasets thus providing more potential for the extraction of detailed information of ground-cover objects (Lu and Weng, 2005; Moran, 2010). In addition, land surface features that occupy minute portions of the Earth's surface can be easily detected and distinguished when such datasets are used (Mariz *et al.*, 2009). Several studies have shown that the use of high spatial resolution produces observations that are at a spatial scale equivalent to field measurements (Goward *et al.*, 2003; Wang *et al.*, 2004; Pacifici *et al.*, 2009). Higher spectral resolution, on the other hand, allows researchers to distinguish subtle variations in reflectance that may occur in similar LULC features such as crops, soils or trees. This can be useful in a number of application areas such as disease mapping or mineral detection. Nonetheless, the use of satellite datasets with high spectral resolution can be problematic due to issues such as signal noise ratio (SNR) or the Hughes phenomenon (Petropoulos *et al.*, 2012a). Despite such shortcomings, advanced machine learning classifiers such as RF which are not sensitive to noise and handle large datasets effectively, can be used to overcome such problems (Chan and Paelinckx, 2008a).

- A large number of studies have shown that the use of spectral information alone can lead to inaccurate interpretations because the difference between land cover objects depends not only on spectral information but also on spatial (contextual) information (Bruzzone *et al.*, 1997; Li and Shao, 2012). For instance, in areas where there is large variation in the spectral response of classes due to high relief and shadow, mapping solely on the basis of spectral response may not be appropriate (Watanachaturaporn *et al.*, 2008). This dissertation therefore recommends that future remote sensing studies focus on incorporating spatial techniques such as texture, slope and shape for more accurate modelling and improvement of LULC classification. These measures provide additional information on neighbouring pixels and therefore enable algorithms to adequately differentiate between different objects on the surface of the Earth.

- It would also be of great practical significance if governmental organizations such as the Department of Environmental Affairs could employ advanced classification techniques for generating more accurate LULC maps. LULC maps are an integral source of information for decision makers and provide the basis for improving land management practices.

## REFERENCES


Adam, E. M., Mutanga, O., Rugege, D., & Ismail, R.(2009). Field spectrometry of papyrus vegetation (Cyperus papyrus L.) in swamp wetlands of St Lucia, South Africa. *In:IEEE International Geoscience and Remote Sensing Symposium (IGARSS)*, Cape Town, South Africa, 260-263.

Adam, E. M., Mutanga, O., Rugege, D., & Ismail, R. (2012). Discriminating the papyrus vegetation (Cyperus papyrus L.) and its co-existent species using random forest and hyperspectral data resampled to HYMAP. *International Journal of Remote Sensing,* 33(2)**,** 552-569.

Adelabu, S., Mutanga, O., Adam, E., & Cho, A. M. (In press). Exploiting Machine Learning Algorithms for Tree Species Classification in a Semi-Arid woodland Using RapidEye image. *Journal of Applied Remote Sensing*.

Al-Ahmadi, F. S., & Hames, A. S. (2008). Comparison of Four Classification Methods to Extract Land Use and Land Cover from Raw Satellite Images for Some Remote Arid Areas, Kingdom of Saudi Arabia. *Earth Science,* 20(1)**,** 167-191.

Anderson, J. R., Hardy, E. E., Roach, J. T., & Witmer, R. E. (1976). *A land use and land cover classification system for use with remote sensor data*, US Government Printing Office.

Bazi, Y., & Melgani, F. (2006). Toward an optimal SVM classification system for hyperspectral remote sensing images. *IEEE Transactions on Geoscience and Remote Sensing,* 44(11)**,** 3374-3385.

Brown, M., Gunn, S. R., & Lewis, H. G. (1999). Support vector machines for optimal classification and spectral unmixing. *Ecological Modelling,* 120(2)**,** 167-179.

Bruzzone, L., Conese, C., Maselli, F., & Roli, F. (1997). Multisource classification of complex rural areas by statistical and neural-network approaches. *Photogrammetric Engineering & Remote Sensing,* 63(5)**,** 523-533.

Chan, J. C.-W., & Paelinckx, D. (2008a). Evaluation of Random Forest and Adaboost tree-based ensemble classification and spectral band selection for ecotope mapping using airborne hyperspectral imagery. *Remote Sensing of Environment,* 112(6)**,** 2999-3011.

Chan, J. C. W., Beckers, P., Spanhove, T., & Borre, J. V. (2012). An evaluation of ensemble classifiers for mapping Natura 2000 heathland in Belgium using spaceborne angular hyperspectral (CHRIS/Proba) imagery. *International Journal of Applied Earth Observation and Geoinformation,* 18**,** 13-22.

Chan, J. C. W., & Paelinckx, D. (2008b). Evaluation of Random Forest and Adaboost tree-based ensemble classification and spectral band selection for ecotope mapping using airborne hyperspectral imagery. *Remote Sensing of Environment,* 112(6)**,** 2999-3011.

Chang, C. I. (2000). An information-theoretic approach to spectral variability, similarity, and discrimination for hyperspectral image analysis. *IEEE Transactions on Information Theory,* 46(5)**,** 1927-1932.

Chapman, D. S., Bonn, A., Kunin, W. E., & Cornell, S. J. (2009). Random Forest characterization of upland vegetation and management burning from aerial imagery. *Journal of Biogeography,* 37(1)**,** 37-46.

Chen, D., & Stow, D. (2003). Strategies for Integrating Information from Multiple Spatial Resolutions into Land-Use/Land-Cover Classification Routines. *Photogrammetric Engineering & Remote Sensing,* 69(11)**,** 1279-1287.

Comber, A. J., Law, A., & Lishman, J. (2004). Application of knowledge for automated land cover change monitoring. *International Journal of Remote Sensing,* 25(16)**,** 3177-3192.

Congalton, R. G. (1991). A review of assessing the accuracy of classifications of remotely sensed data. *Remote Sensing of Environment,* 37(1)**,** 35-46.

Dalton, J. B., Bove, D. J., Mladinich, C. S., & Rockwell, B. W. (2004). Identification of spectrally similar materials using the USGS Tetracorder algorithm: the calcite–epidote–chlorite problem. *Remote Sensing of Environment,* 89(4)**,** 455-466.

Daughtry, C. S. (2001). Discriminating crop residues from soil by shortwave infrared reflectance. *Agronomy Journal,* 93(1)**,** 125-131.

DeFries, R., & Chan, J. C. W. (2000). Multiple criteria for evaluating machine learning algorithms for land cover classification from satellite data. *Remote Sensing of Environment,* 74(3)**,** 503-515.

Dixon, B., & Candade, N. (2008). Multispectral landuse classification using neural networks and support vector machines: one or the other, or both? *International Journal of Remote Sensing,* 29(4)**,** 1185-1206.

Duro, D. C., Franklin, S. E., & Dubé, M. G. (2012). A comparison of pixel-based and object-based image analysis with selected machine learning algorithms for the classification of agricultural landscapes using SPOT-5 HRG imagery. *Remote Sensing of Environment,* 118**,** 259-272.

Dye, M., Mutanga, O., & Ismail, R. (2011). Examining the utility of random forest and AISA Eagle hyperspectral image data to predict Pinus patula age in KwaZulu-Natal, South Africa. *Geocarto International,* 26(4)**,** 275-289.

Dye, M., Mutanga, O., & Ismail, R. (2012). Combining spectral and textural remote sensing variables using random forests: predicting the age of Pinus patula forests in KwaZulu-Natal, South Africa. *Journal of Spatial Science,* 57(2)**,** 193-211.

ENVI (2006). *Atmospheric Correction Module: QUAC and FLAASH User's Guide,* Boulder, Colorado, USA: ITT Visual Information Solutions.

Ezemvelo, W. (2005). KZNSCP: Land-Cover dataset. *Biodiversity GIS*.

Fang, S., Gertner, G., Wang, G., & Anderson, A. (2006). The impact of misclassification in land use maps in the prediction of landscape dynamics. *Landscape ecology,* 21(2)**,** 233-242.

Feleke, A. K. (2010). *Land use and land cover in relation to Chromolaena odorata distribution: Mapping and change detection in St Lucia wetland area* MSc, University of Twente.

Foody, G. M. (2004). Thematic map comparison: evaluating the statistical significance of differences in classification accuracy. *Photogrammetric engineering and remote sensing,* 70(5)**,** 627-634.

Foody, G. M. (2009a). Classification accuracy comparison: hypothesis tests and the use of confidence intervals in evaluations of difference, equivalence and non-inferiority. *Remote Sensing of Environment,* 113(8)**,** 1658-1663.

Foody, G. M. (2009b). Sample size determination for image classification accuracy assessment and comparison. *International Journal of Remote Sensing,* 30(20)**,** 5273-5291.

Foody, G. M., & Mathur, A. (2004a). A relative evaluation of multiclass image classification by support vector machines. *IEEE Transactions on Geoscience and Remote Sensing,* 42(6)**,** 1335-1343.

Foody, G. M., & Mathur, A. (2004b). Toward intelligent training of supervised image classifications: directing training data acquisition for SVM classification. *Remote Sensing of Environment,* 93(1)**,** 107-117.

Friedl, M. A., & Brodley, C. E. (1997). Decision tree classification of land cover from remotely sensed data. *Remote sensing of environment,* 61(3)**,** 399-409.

Ghimire, B., Rogan, J., & Miller, J. (2010). Contextual land-cover classification: incorporating spatial dependence in land-cover classification models using random forests and the Getis statistic. *Remote Sensing Letters,* 1(1)**,** 45-54.

Ghose, M., Pradhan, R., & Ghose, S. S. (2010). Decision Tree Classification of Remotely Sensed Satellite Data using Spectral Separability Matrix. *International Journal of Advanced Computer Science and Applications,* 1(5)**,** 93-101.

Gislason, P. O., Benediktsson, J. A., & Sveinsson, J. R. (2006). Random Forests for land cover classification. *Pattern Recognition Letters,* 27(4)**,** 294-300.

Goward, S. N., Davis, P. E., Fleming, D., Miller, L., & Townshend, J. R. (2003). Empirical comparison of Landsat 7 and IKONOS multispectral measurements for selected Earth Observation System (EOS) validation sites. *Remote Sensing of Environment,* 88(1)**,** 80-99.

Guo, L., Chehata, N., Mallet, C., & Boukir, S. (2011). Relevance of airborne lidar and multispectral image data for urban scene classification using Random Forests. *ISPRS Journal of Photogrammetry and Remote Sensing,* 66(1)**,** 56-66.

Haack, B., & English, R. (1996). National land cover mapping by remote sensing. *World Development,* 24(5)**,** 845-855.

Ham, J., Chen, Y., Crawford, M. M., & Ghosh, J. (2005). Investigation of the random forest framework for classification of hyperspectral data. *IEEE Transactions on Geoscience and Remote Sensing,* 43(3)**,** 492-501.

Hermes, L., Frieauff, D., Puzicha, J., & Buhmann, J. M.(1999). Support vector machines for land usage classification in Landsat TM imagery. *In:IEEE International Geoscience and Remote Sensing Symposium (IGARSS)* 348-350.

Huang, C., Davis, L., & Townshend, J. (2002). An assessment of support vector machines for land cover classification. *International Journal of Remote Sensing,* 23(4)**,** 725-749.

Immitzer, M., Atzberger, C., & Koukal, T. (2012). Tree Species Classification with Random Forest Using Very High Spatial Resolution 8-Band WorldView-2 Satellite Data. *Remote Sensing,* 4(9)**,** 2661-2693.

Ismail, R., & Mutanga, O. (2010). A comparison of regression tree ensembles: Predicting *Sirex noctilio* induced water stress in *Pinus patula* forests of KwaZulu-Natal, South Africa. *International Journal of Applied Earth Observation and Geoinformation,* 12**,** S45-S51.

Jia, K., Wu, B., Tian, Y., Li, Q., & Du, X. (2011). Spectral discrimination of opium poppy using field spectrometry. *IEEE Transactions on Geoscience and Remote Sensing,* 49(9)**,** 3414-3422.

Johnson, R. M., Viator, R. P., Veremis, J. C., Richard Jr, E. P., & Zimba, P. V. (2008). Discrimination of sugarcane varieties with pigment profiles and high resolution, hyperspectral leaf reflectance data. *Journal Association Sugar Cane Technologists,* 28**,** 63-75.

Kavzoglu, T. (2009). Increasing the accuracy of neural network classification using refined training data. *Environmental Modelling & Software,* 24(7)**,** 850-858.

Kavzoglu, T., & Colkesen, I. (2009). A kernel functions analysis for support vector machines for land cover classification. *International Journal of Applied Earth Observation and Geoinformation,* 11(5)**,** 352-359.

Kavzoglu, T., & Mather, P. (2003). The use of backpropagating artificial neural networks in land cover classification. *International Journal of Remote Sensing,* 24(23)**,** 4907-4938.

Lawrence, R. L., Wood, S. D., & Sheley, R. L. (2006). Mapping invasive plants using hyperspectral imagery and Breiman Cutler classifications (RandomForest). *Remote Sensing of Environment,* 100(3)**,** 356-362.

Li, C., & Shao, G. (2012). Object-oriented classification of land use/cover using digital aerial orthophotography. *International Journal of Remote Sensing,* 33(4)**,** 922-938.

Lillesand, T. M., Kiefer, R. W., & Chipman, J. W. (2008). *Remote sensing and image interpretation*, John Wiley & Sons Ltd.

Loosvelt, L., Peters, J., Skriver, H., Lievens, H., Van Coillie, F., De Baets, B., & Verhoest, N. E. C. (2012). Random Forests as a tool for estimating uncertainty at pixel-level in SAR image classification. *International Journal of Applied Earth Observation and Geoinformation,* 19**,** 173-184.

Loveland, T., Reed, B., Brown, J., Ohlen, D., Zhu, Z., Yang, L., & Merchant, J. (2000). Development of a global land cover characteristics database and IGBP DISCover from 1 km AVHRR data. *International Journal of Remote Sensing,* 21(6-7)**,** 1303-1330.

Lu, D., & Weng, Q. (2004). Spectral mixture analysis of the urban landscape in Indianapolis with Landsat ETM+ imagery. *Photogrammetric engineering and remote sensing,* 70(9)**,** 1053-1062.

Lu, D., & Weng, Q. (2005). Urban classification using full spectral information of Landsat ETM+ imagery in Marion County, Indiana. *Photogrammetric Engineering and Remote Sensing*, 71(11)**,** 1275-1284.

Lu, D., & Weng, Q. (2007). A survey of image classification methods and techniques for improving classification performance. *International Journal of Remote Sensing*, 28(5)**,** 823-870.

Mafuratidze, P. (2010). *Discriminating wetland vegetation species in an African savanna using hyperspectral data*. MSc thesis, University of KwaZulu-Natal.

Mahdavi, A. (2010). IRS-1C image data applications for land use/land cover mapping in Zagros region, Case study: Ilam watershed, West of Iran. *Caspian Journal of Environmental Science*, 8(1)**,** 35-41.

Manandhar, R., Odeh, I. O., & Ancev, T. (2009). Improving the accuracy of land use and land cover classification of Landsat data using post-classification enhancement. *Remote Sensing*, 1(3)**,** 330-344.

Mansour, K., Mutanga, O., Everson, T., & Adam, E. (2012). Discriminating indicator grass species for rangeland degradation assessment using hyperspectral data resampled to AISA Eagle resolution. *ISPRS Journal of Photogrammetry and Remote Sensing*, 70**,** 56-65.

Marchisio, G., Pacifici, F., & Padwick, C.(2010). On the relative predictive value of the new spectral bands in the WorldWiew-2 sensor. *In: IEEE International Geoscience and Remote Sensing Symposium (IGARSS)*, 2723-2726.

Mariz, C., Gianelle, D., Bruzzone, L., & Vescovo, L. (2009). Fusion of multi-spectral SPOT-5 images and very high resolution texture information extracted from digital orthophotos for automatic classification of complex Alpine areas. *International journal of remote sensing*, 30(11)**,** 2859-2873.

Mather, P. M., & Koch, M. (2011). *Computer processing of remotely sensed images: An introduction*, John Wiley & Sons Ltd.

Mathur, A., & Foody, G. M. (2008). Multiclass and binary SVM classification: implications for training and classification users. *IEEE Geoscience and Remote Sensing Letters*, 5(2)**,** 241-245.

Melgani, F., & Bruzzone, L. (2004). Classification of hyperspectral remote sensing images with support vector machines. *IEEE Transactions on Geoscience and Remote Sensing*, 42(8)**,** 1778-1790.

Metternicht, G., & Zinck, J. (1997). Spatial discrimination of salt-and sodium-affected soil surfaces. *International Journal of Remote Sensing*, 18(12)**,** 2571-2586.

Mingjie, L., Xiyong, H., Mingming, Z., & Chunyan, S.(2010). Extraction and application of impervious surface area in Yellow River Delta. *In:Second IITA International Conference on Geoscience and Remote Sensing (IITA-GRS)*, 634-637.

Moran, E. F. (2010). Land cover classification in a complex urban-rural landscape with Quickbird imagery. *Photogrammetric engineering and remote sensing*, 76(10)**,** 1159.

Mountrakis, G., Im, J., & Ogole, C. (2011). Support vector machines in remote sensing: A review. *ISPRS Journal of Photogrammetry and Remote Sensing,* 66(3)**,** 247-259.

Mutanga, O., Adam, E., & Cho, M. A. (2012). High density biomass estimation for wetland vegetation using WorldView-2 imagery and random forest regression algorithm. *International Journal of Applied Earth Observation and Geoinformation,* 18**,** 399-406.

Na, X., Zang, S., & Wang, J.(2009). Evalution of random forest ensemble classification for land cover mapping using TM and ancillary geographical data. *In:Sixth International Conference on Fuzzy Systems and Knowledge Discovery,* 89-93.

Navulur, K. (2009). The Benefits of the 8 Spectral Bands of WorldView-2: White paper. Available: http://www.digitalglobe.com [Accessed 18 April 2013].

Novack, T., Esch, T., Kux, H., & Stilla, U. (2011). Machine learning comparison between WorldView-2 and QuickBird-2-simulated imagery regarding object-based urban land cover classification. *Remote Sensing,* 3(10)**,** 2263-2282.

Ojo, A. G., & Adesina, F. A.(2010). An assessment of the efficiency of Landsat, Nigeriasat-1 and Spot images for landuse/landcover analyses in Ekiti West area of Nigeria. *In:ISPRS TC VII Symposium* 5-7 July Vienna, Austria, 430-435.

Ok, A. O., Akar, O., & Gungor, O. (2012). Evaluation of random forest method for agricultural crop classification. *European Journal of Remote Sensing,* 45**,** 421-432.

Ozdemir, I., & Karnieli, A. (2011). Predicting forest structural parameters using the image texture derived from WorldView-2 multispectral imagery in a dryland forest, Israel. *International Journal of Applied Earth Observation and Geoinformation,* 13(5)**,** 701-710.

Pacifici, F. (2011). Very High Spatial Resolution Imagery for Urban Applications. Available: http://www.earthzine.org/ [Accessed 10 June 2013].

Pacifici, F., Chini, M., & Emery, W. J. (2009). A neural network approach using multi-scale textural metrics from very high-resolution panchromatic imagery for urban land-use classification. *Remote Sensing of Environment,* 113(6)**,** 1276-1292.

Pal, M. (2005). Random forest classifier for remote sensing classification. *International Journal of Remote Sensing,* 26(1)**,** 217-222.

Pal, M. (2006). Support vector machine-based feature selection for land cover classification: a case study with DAIS hyperspectral data. *International Journal of Remote Sensing,* 27(14)**,** 2877-2894.

Pal, M., & Mather, P. (2004). Assessment of the effectiveness of support vector machines for hyperspectral data. *Future Generation Computer Systems,* 20(7)**,** 1215-1225.

Peerbhay, K., Y., Mutanga, O., & Ismail, R. (In press). Investigating the capability of few strategically placed WorldView-2 multispectral bands to discriminate forest species in KwaZulu-Natal, South Africa. *IEEE JOURNAL OF SELECTED TOPICS IN APPLIED EARTH OBSERVATIONS AND REMOTE SENSING.*

Peerbhay, K. Y., Mutanga, O., & Ismail, R. (2013). Commercial tree species discrimination using airborne AISA Eagle hyperspectral imagery and partial least squares discriminant analysis (PLS-DA) in KwaZulu–Natal, South Africa. *ISPRS Journal of Photogrammetry and Remote Sensing,* 79**,** 19-28.

Perumal, K., & Bhaskaran, R. (2010). Supervised classification performance of multispectral images. *JOURNAL OF COMPUTING,* 2(2)**,** 124-129.

Peters, J., Baets, B. D., Verhoest, N. E., Samson, R., Degroeve, S., Becker, P. D., & Huybrechts, W. (2007). Random forests as a tool for ecohydrological distribution modelling. *Ecological Modelling,* 207(2)**,** 304-318.

Peters, J., Van Coillie, F., Westra, T., & De Wulf, R. (2011). Synergy of very high resolution optical and radar data for object-based olive grove mapping. *International Journal of Geographical Information Science,* 25(6)**,** 971-989.

Petropoulos, G. P., Arvanitis, K., & Sigrimis, N. (2012a). Hyperion hyperspectral imagery analysis combined with machine learning classifiers for land use/cover mapping. *Expert Systems with Applications,* 39(3)**,** 3800-3809.

Petropoulos, G. P., Kalaitzidis, C., & Prasad Vadrevu, K. (2012b). Support vector machines and object-based classification for obtaining land-use/cover cartography from Hyperion hyperspectral imagery. *Computers & Geosciences,* 41**,** 99-107.

Pontius Jr, R. G., & Millones, M. (2011). Death to Kappa: birth of quantity disagreement and allocation disagreement for accuracy assessment. *International Journal of Remote Sensing,* 32(15)**,** 4407-4429.

Prasad, A. M., Iverson, L. R., & Liaw, A. (2006). Newer classification and regression tree techniques: bagging and random forests for ecological prediction. *Ecosystems,* 9(2)**,** 181-199.

Puetz, A. M., Lee, K., & Olsen, R. C.(2009). WorldView-2 data simulation and analysis results. *In:SPIE Defense, Security, and Sensing*, 73340U-73340U-9.

Pugh, M. L., & Waxman, A. M.(2006). Classification of spectrally-similar land cover using multi-spectral neural image fusion and the fuzzy artmap neural classifier. *In: IEEE International Conference on Geoscience and Remote Sensing Symposium (IGARSS)*, 1808-1811.

Ribeiro, G., & Garcia Fonseca, L.(2013). Urban land cover classification using worldview-2 images and C4. 5 algorithm. *In:Urban Remote Sensing Event (JURSE), ,* 250-253.

Richards, J. A. (2006). *Remote sensing digital image analysis*, Springer.

Rodríguez-Galiano, V. F., Chica-Olmo, M., Abarca-Hernandez, F., Atkinson, P., & Jeganathan, C. (2012b). Random Forest classification of Mediterranean land cover using multi-seasonal imagery and multi-seasonal texture. *Remote Sensing of Environment*, 121**,** 93-107.

Rodriguez-Galiano, V. F., Ghimire, B., Rogan, J., Chica-Olmo, M., & Rigol-Sanchez, J. (2012a). An assessment of the effectiveness of a random forest classifier for land-cover classification. *ISPRS Journal of Photogrammetry and Remote Sensing,* 67**,** 93-104.

Rogan, J., & Chen, D. M. (2004). Remote sensing technology for mapping and monitoring land-cover and land-use change. *Progress in Planning,* 61(4)**,** 301-325.

Salberg, A. B., & Jenssen, R. (2012). Land-cover classification of partly missing data using support vector machines. *International Journal of Remote Sensing,* 33(14)**,** 4471-4481.

Sesnie, S. E., Finegan, B., Gessler, P. E., Thessler, S., Bendana, Z. R., & Smith, A. M. S. (2010). The multispectral separability of Costa Rican rainforest types with support vector machines and Random Forest decision trees. *International Journal of Remote Sensing,* 31(11)**,** 2885-2909.

Song, M., Civco, D., & Hurd, J. (2005). A competitive pixel-object approach for land cover classification. *International Journal of Remote Sensing,* 26(22)**,** 4981-4997.

Song, S., Gong, W., Zhu, B., & Huang, X. (2011). Wavelength selection and spectral discrimination for paddy rice, with laboratory measurements of hyperspectral leaf reflectance. *ISPRS Journal of Photogrammetry and Remote Sensing,* 66(5)**,** 672-682.

Song, X., Duan, Z., & Jiang, X. (2012). Comparison of artificial neural networks and support vector machine classifiers for land cover classification in Northern China using a SPOT-5 HRG image. *International Journal of Remote Sensing,* 33(10)**,** 3301-3320.

Stumpf, A., & Kerle, N. (2011). Object-oriented mapping of landslides using Random Forests. *Remote sensing of environment,* 115(10)**,** 2564-2577.

Tan, K., Lim, H., & Jafri, M. Z. M.(2011). Comparison of Neural Network and Maximum Likelihood classifiers for land cover classification using landsat multispectral data. *In:IEEE Conference on Open Systems (ICOS),* 241-244.

Van Aardt, J. A. (2000). Spectral separability among six southern tree species. *Photogrammetric Engineering & Remote Sensing,* 67(12)**,** 1367-1375.

Vivier, L., Cyrus, D., Owen, R., & Jerling, H. (2010). Fish assemblages in the Mfolozi–Msunduzi estuarine system, KwaZulu-Natal, South Africa, when not linked to the St Lucia mouth. *African Journal of Aquatic Science,* 35(2)**,** 141-154.

Walton, J. T. (2008). Subpixel urban land cover estimation: comparing cubist, random forests, and support vector regression. *Photogrammetric Engineering & Remote Sensing,* 74(10)**,** 1213-1222.

Wang, L., Sousa, W. P., Gong, P., & Biging, G. S. (2004). Comparison of IKONOS and QuickBird images for mapping mangrove species on the Caribbean coast of Panama. *Remote Sensing of Environment,* 91(3)**,** 432-440.

Waske, B., Benediktsson, J. A., Árnason, K., & Sveinsson, J. R. (2009). Mapping of hyperspectral AVIRIS data using machine-learning algorithms. *Canadian Journal of Remote Sensing,* 35(1)**,** 106-116.

Waske, B., & Braun, M. (2009). Classifier ensembles for land cover mapping using multitemporal SAR imagery. *ISPRS Journal of Photogrammetry and Remote Sensing,* 64(5)**,** 450-457.

Watanachaturaporn, P., Arora, M. K., & Varshney, P. K. (2008). Multisource classification using support vector machines: An empirical comparison with decision tree and neural network classifiers. *Photogrammetric Engineering and Remote Sensing,* 74(2)**,** 239-246.

Watts, J. D., & Lawrence, R. L. (2008). Merging random forest classification with an object-oriented approach for analysis of agricultural lands. *The International Archives of the Photogrammetry, Remote Sensing and Spatial Information Sciences,* 37**,** 579-582.

Watts, J. D., Lawrence, R. L., Miller, P. R., & Montagne, C. (2009). Monitoring of cropland practices for carbon sequestration purposes in north central Montana by Landsat remote sensing. *Remote Sensing of Environment,* 113(9)**,** 1843-1852.

Wolf, A. (2010). Using WorldView 2 Vis-NIR MSI imagery to support land mapping and feature extraction using normalized difference index ratios. *DigitalGlobe 8-Band Research Challenge***,** 1-13.

Wulder, M. A., & Franklin, S. E. (2003). *Remote sensing of forest environments: concepts and case studies,* Springer.

Yuan, F., Bauer, M. E., Heinert, N. J., & Holden, G. R. (2005). Multi-level land cover mapping of the Twin Cities (Minnesota) metropolitan area with multi-seasonal Landsat TM/ETM+ data. *Geocarto International,* 20(2)**,** 5-13.

Zengeya, F. M., Mutanga, O., & Murwira, A. (2012). Linking remotely sensed forage quality estimates from WorldView-2 multispectral data with cattle distribution in a savanna landscape. *International Journal of Applied Earth Observation and Geoinformation,* 21**,** 513-524.

Zhang, J., & Kerekes, J.(2011). Unsupervised urban land-cover classification using WorldView-2 data and self-organizing maps. *In:Geoscience and Remote Sensing Symposium (IGARSS), 2011 IEEE International*, 24-29 July 2011. 201-204.

Zhou, X., Jancso, T., Chen, C., & Verone, M. W.(2012). Urban Land Cover Mapping Based on Object Oriented Classification Using WorldView 2 Satellite Remote Sensing Images. *In:International Scientific Conference on Sustainable Development & Ecological Footprint* 26-27 March Sopron, Hungary, 1-10.